Received: 10 January 2024 | Accepted: 25 September 2024

DOI: 10.1002/ajb2.16451

American Journal of Botany

RESEARCH ARTICLE

Toward a phylogenomic classification of magnoliids

Andrew J. Helmstetter[1,2] | **Zacky Ezedin**[3,4] | **Elton John de Lírio**[5,6] | **Sylvia M. de Oliveira**[7] | **Lars W. Chatrou**[8] | **Roy H. J. Erkens**[7,9,10] | **Isabel Larridon**[8,11] | **Kevin Leempoel**[11] | **Olivier Maurin**[11,12] | **Shyamali Roy**[11] | **Alexandre R. Zuntini**[11] | **William J. Baker**[11,13] | **Thomas L. P. Couvreur**[7,14] | **Félix Forest**[11] | **Hervé Sauquet**[15,16]

Correspondence

Hervé Sauquet, National Herbarium of NSW, Botanic Gardens of Sydney, Locked Bag 6002, Mount Annan, NSW 2567, Australia.
Email: herve.sauquet@botanicgardens.nsw.gov.au

Andrew J. Helmstetter, Institut des Sciences de l'Évolution de Montpellier (ISEM), Université de Montpellier, campus Triolet, 34095 Montpellier cedex 05.
Email: andrew.j.helmstetter@gmail.com

Abstract

Premise: Magnoliids are a strongly supported clade of angiosperms. Previous phylogenetic studies based primarily on analyses of a limited number of mostly plastid markers have led to the current classification of magnoliids into four orders and 18 families. However, uncertainty remains regarding the placement of several families.

Methods: For the first comprehensive phylogenomic analysis of magnoliids as a whole, we sampled 235 species from 199 (74%) genera and representing all families and most subfamilies and tribes. We analyzed newly generated data from the Angiosperms353 probe set using both coalescent and concatenation analyses and testing the impact of multiple filtering and alignment strategies.

Results: While our results generally provide further support for previously established phylogenetic relationships in both magnoliids as a whole and large families including Annonaceae and Lauraceae, they also provide new evidence for previously ambiguous relationships. In particular, we found support for the position of Hydnoraceae as sister to the remainder of Piperales, though evidence was conflicting, and resolved the backbone of relationships among most genera of Myristicaceae. Different analytical strategies tended to have rather small effects on branch support and topology.

Conclusions: Although some of our results are limited by low gene recovery for a number of taxa and significant gene tree conflict for some relationships, this study represents a significant step toward reconstructing the evolutionary history of a major lineage of angiosperms. Based on these results, we present an updated phylogenetic classification for magnoliids, recognizing 21 families, summarizing previously established subfamilies and tribes, and describing new tribes for Myristicaceae.

KEYWORDS

Angiosperms353, Canellales, Laurales, Magnoliales, magnoliids, phylogenetic classification, phylogenomics, Piperales

Magnoliids (sensu APG II, 2003; APG III, 2009; APG IV, 2016; Magnoliidae sensu Cantino et al., 2007; Soltis et al., 2011; Magnolianae sensu Chase and Reveal, 2009) are a large clade of angiosperms consisting of approximately 12,000 species assigned to 18 families and four orders (Massoni et al., 2014; APG IV, 2016; Stevens, 2022). Magnoliids diverged early from other major lineages of angiosperms (including monocots, eudicots, *Amborella*, Nymphaeales,

---

For affiliations refer to page 18.

William J. Baker, Thomas L.P. Couvreur, Félix Forest and Hervé Sauquet are joint senior authors.

Austrobaileyales, Chloranthaceae, and *Ceratophyllum*). Indeed, magnoliids can be traced in the fossil record to at least the Barremian (ca. 121–129 Ma; Massoni et al., 2015), and fossil-calibrated molecular dating studies have estimated the stem age of the clade to fall between 133 and 242 Ma (Magallón et al., 2015; Ramírez-Barahona et al., 2020; Zuntini et al., 2024). Species of magnoliids are found across a broad range of habitats and climates, but occur predominantly in tropical and warm temperate rain forests. The group has long been noted for its diverse and unusual flower morphology (Figures 1, 2; Endress, 1987), differing from most species of monocots and eudicots particularly in their numbers of organ parts and whorls. These features, along with other uncommon traits and their fossil record, had led to theories that some living members of the group may resemble ancestors of angiosperms as a whole (Cronquist, 1981). Although many questions remain, phylogenetic analyses of morphological evolution have consistently rejected this idea (Sauquet et al., 2003, 2017, 2018; Endress and Doyle, 2009, 2015).

Numerous studies at various scales conducted over the last three decades have led to an increasingly robust and well-supported backbone for phylogenetic relationships among families of magnoliids (Qiu et al., 1999; Doyle and Endress, 2000; Sauquet et al., 2003; Moore et al., 2007; Soltis et al., 2011; Massoni et al., 2014; Wickett et al., 2014; Li et al., 2019; One Thousand Plant Transcriptomes Initiative, 2019; Zuntini et al., 2024). Briefly, these studies have supported the monophyly of the four orders as initially recircumscribed by the Angiosperm Phylogeny Group (APG, 1998; APG II, 2003), with two sister clades, one comprising Canellales and Piperales and the other Laurales and Magnoliales. Relationships within orders have become relatively stable as well, but important questions persist. In particular, much uncertainty remains in Piperales regarding the relationship between the two traditional lineages of Aristolochiaceae (subfamilies Asaroideae and Aristolochioideae) and two enigmatic taxa (subfamily Hydnoroideae and *Lactoris*) (Naumann et al., 2013; Massoni et al., 2014; Jost et al., 2021). In Laurales, no consensus has emerged yet on the relationships among the three largest families, Lauraceae, Hernandiaceae, and Monimiaceae (Doyle and Endress, 2000; Renner and Chanderbali, 2000; Massoni et al., 2014). In Magnoliales, the position of Magnoliaceae in relation to the other families of the order also continues to be equivocal (Doyle and Endress, 2000; Sauquet et al., 2003; Massoni et al., 2014). Lastly, considerable progress has been made in reconstructing the phylogenetic backbones of two of the largest families, Annonaceae (Chatrou et al., 2012; Guo et al., 2017; Couvreur et al., 2019) and Piperaceae (Jaramillo et al., 2004; Wanke et al., 2007a, b; Smith et al., 2008). In contrast, the global phylogeny of Lauraceae is only now becoming more confidently resolved (Song et al., 2020), and very few studies have addressed relationships among genera in two smaller families, Monimiaceae (Renner et al., 2010) and Myristicaceae (Sauquet et al., 2003; Massoni et al., 2014; Frost et al., 2022).

Here we took advantage of recent technological advances in plant nuclear phylogenomics to further explore phylogenetic relationships among genera and families of magnoliids. Specifically, we used a target enrichment strategy with the universal Angiosperms353 probe set (Johnson et al., 2019; Baker et al., 2022). To date, a single clade-specific probe set has been designed in magnoliids, for Annonaceae (Couvreur et al., 2019). However, there is growing evidence that universal probes may be as effective as clade-specific probes (Larridon et al., 2020; Shah et al., 2021; Fonseca et al., 2024), and the benefits of community convergence around a standard gene set are well documented (Baker et al., 2021; McDonnell et al., 2021). Our goal here was to capitalize on the unique opportunity created by the extensive sequencing of magnoliid genera undertaken jointly by the Plant and Fungal Trees of Life (PAFTOL) project (Baker et al., 2022; Zuntini et al., 2024) and the Genomics for Australian Plants (GAP) project, and evaluate the utility of these new data to further test and address long-standing questions remaining about the phylogenetic backbone of magnoliids.

Phylogenomic data contain inherent uncertainties (e.g., variable recovery) and present new analytical challenges, leading to the risk that specific filtering or analytical decisions may impact results, particularly when estimating trees across large evolutionary scales, as is the case for magnoliids. Therefore, we also aimed to examine the impact of multiple data filtering strategies on phylogenomic reconstruction, tree topology, and associated measures of branch support. We varied the way loci were selected, the type of data (exons only vs introns and exons), the sequence alignment method, the sequence trimming algorithm, and the method of phylogenetic inference. In this way, we were able to test the robustness of the relationships recovered and the effect of varying different steps in the phylogenomic pipeline, which has rarely been examined in classic phylogenomic studies.

While our results broadly corroborate and add support to most of the relationships that had emerged previously, we also found new evidence for the positions of Lauraceae and Magnoliaceae and a distinct placement for Hydnoraceae not previously retrieved. We also resolved most relationships among genera in Myristicaceae, which had proven difficult to reconstruct so far (but see Frost et al., 2022). Based on this new study and previous work in selected families, we propose an updated phylogenetic classification for magnoliids as a whole.

MATERIALS AND METHODS

Taxon sampling

Our sampling consisted of 238 taxa representing 235 unique species, 199 genera, and all 18 families of Canellales, Laurales, Magnoliales, and Piperales, with a respective generic representation of 90% (9/10), 71% (75/106), 74% (101/136) and 88% (14/16) according to the revised list of genera presented at the end of this paper. In addition, we used six specimens sampled from the four genera of

FIGURE 1 Floral diversity in Canellales, Piperales, and Laurales. (A) Canellaceae: *Canella winterana* (L.) Gaertn.; (B) Winteraceae, Winteroideae: *Drimys lanceolata* (Poir.) Baill.; (C) Hydnoraceae, *Hydnora visseri* Bolin, E. Maass & Musselman; (D) Asaraceae: *Asarum europaeum* L.; (E) Aristolochiaceae: *Aristolochia gigantea* Mart. & Zucc.; (F) Saururaceae: *Houttuynia cordata* Thunb.; (G) Piperaceae, Piperoideae: *Peperomia tetraphylla* (G. Forst.) Hook. & Arn.; (H) Calycanthaceae, Calycanthoideae: *Calycanthus occidentalis* Hook. & Arn.; (I) Calycanthaceae, Idiospermoideae: *Idiospermum australiense* (Diels) S.T. Blake; (J) Siparunaceae: *Glossocalyx longicuspis* Benth.; (K) Gomortegaceae: *Gomortega keule* (Molina) Baill.; (L) Atherospermataceae: *Doryphora sassafras* Endl.; (M) Monimiaceae, Monimioideae: *Peumus boldus* Molina; (N) Lauraceae, Hypodaphnideae: *Hypodaphnis zenkeri* (Engl.) Stapf; (O) Lauraceae, Laureae: *Persea americana* L. Photo credits: (A) Kevin Nixon (http://www.diversityoflife.org/); (B, D, E, G–I, L–O): Hervé Sauquet; (C) Julia Naumann; (F) Laetitia Carrive; (J) Thomas L.P. Couvreur; (K) Ana Almeida.

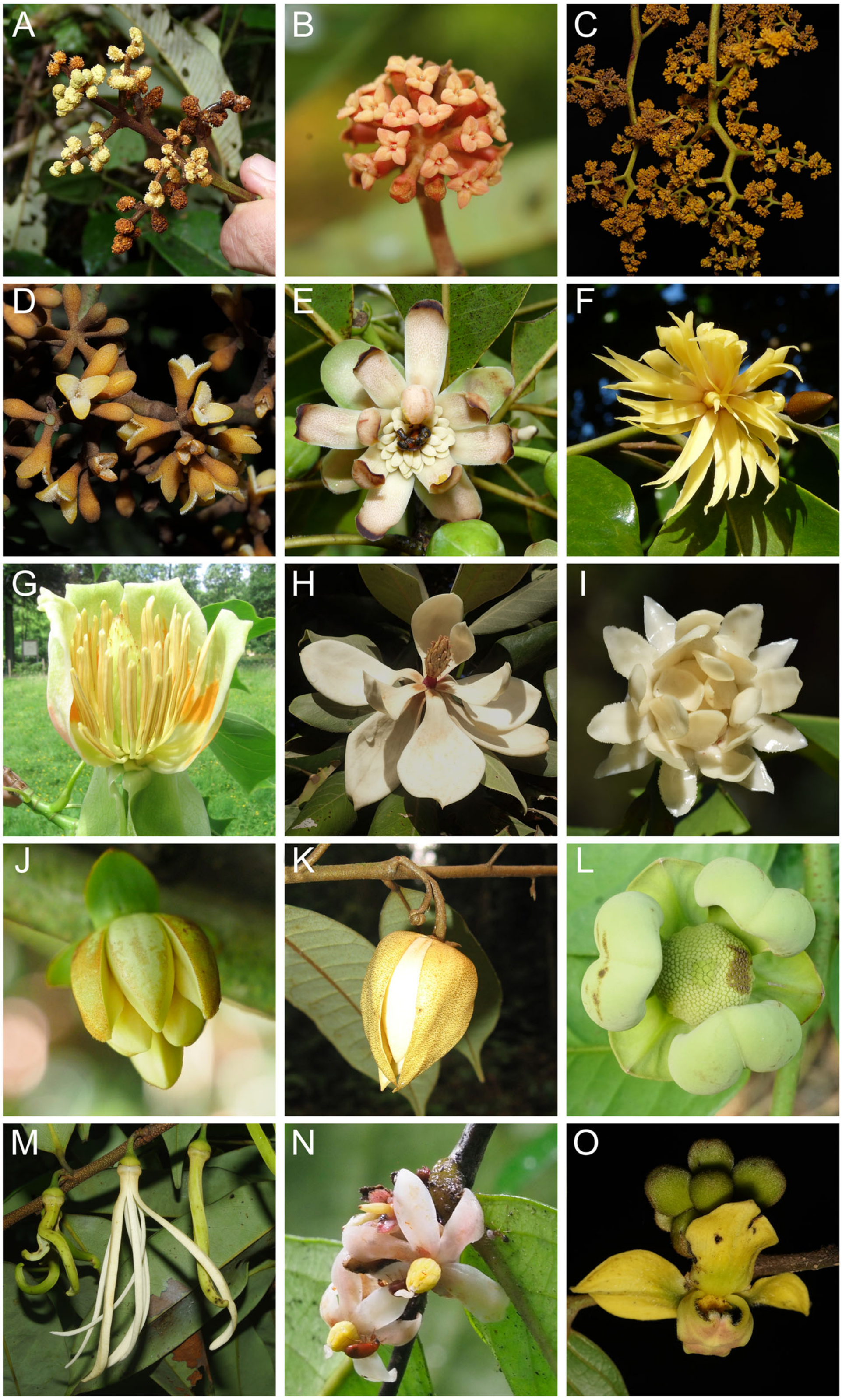

FIGURE 2 Floral diversity in Magnoliales. (A) Myristicaceae, Mauloutchieae: *Pycnanthus angolensis* (Welw.) Warb.; (B) Myristicaceae, Scyphocephalieae: *Scyphocephalium mannii* (Benth.) Warb.; (C) Myristicaceae, Horsfieldieae: *Horsfieldia sylvestris* (Houtt.) Warb.; (D) Myristicaceae, Viroleae: *Virola sebifera* Aubl.; (E) Degeneriaceae: *Degeneria vitiensis* I.W. Bailey & A.C. Sm.; (F) Himantandraceae: *Galbulimima baccata* F.M. Bailey; (G) Magnoliaceae: *Liriodendron tulipifera* L.; (H) Magnoliaceae: *Magnolia sororum* Seibert; (I) Eupomatiaceae: *Eupomatia laurina* R. Br.; (J) Annonaceae, Anaxagoreoideae: *Anaxagorea brevipes* Benth.; (K) Annonaceae, Ambavioideae: *Meiocarpidium oliverianum* (Baill.) D.M. Johnson & N.A. Murray; (L) Annonaceae, Annonoideae: *Cymbopetalum baillonii* R.E. Fr.; (M) Annonaceae, Annonoideae: *Xylopia aethiopica* (Dunal) A. Rich.; (N) Annonaceae, Malmeoideae: *Sirdavidia solannona* Couvreur & Sauquet; (O) Annonaceae, Malmeoideae: *Mitrephora diversifolia* (Span.) Miq. Photo credits: (A, E, F, I): Hervé Sauquet; (B, D, G, J–N) Thomas L.P. Couvreur; (C, H, O) Zacky Ezedin.

Chloranthaceae (Chloranthales) as outgroup taxa in phylogenetic analyses, a choice supported by most recent phylogenomic analyses of nuclear data (One Thousand Plant Transcriptomes Initiative, 2019; Baker et al., 2022; Zuntini et al., 2024).

Samples for this study were obtained from five distinct sources. The vast majority (191) were new sequence data generated for this study as part of the broader PAFTOL project (Baker et al., 2022; Zuntini et al., 2024). Another 20 taxa from Australia were new sequence data contributed by the GAP project, and six additional taxa were sourced from a project on Neotropical Myristicaceae led by one of us (SMDO). Lastly, we also used previously published sequence data for 22 taxa from the One Thousand Plant Transcriptomes (1KP) Initiative (2019) and five from the NCBI Sequence Read Archive (SRA; https://www.ncbi.nlm.nih.gov/sra). All voucher and source details are provided in Appendix S1.

DNA extraction, library preparation, and sequencing

For PAFTOL samples, we extracted DNA using a modified CTAB protocol (Doyle and Doyle, 1987), then purified it using Mag-Bind TotalPure NGS magnetic beads (Omega Bio-tek, Norcross, GA, USA). We then assessed the average fragment size within each extraction using a 1.5× agarose gel and quantified the amount of double-stranded DNA using a Qubit 3.0 fluorometer (ThermoFisher Scientific, Waltham, MA, USA). When average fragment size was longer than 350 bp, extracts were sonicated with a M220 Focused-ultrasonicator with microTUBEs AFA Fiber Pre-Slit Snap-Cap (Covaris, Woburn, MA, USA) following the manufacturer's protocol to generate ~350 bp insert sizes.

We prepared dual-indexed libraries with Dual Index Primers Set 1, NEBNext Multiplex Oligos for Illumina (New England BioLabs, Ipswich, MA, USA) using DNA NEBNext UltraTM II Library Prep Kits at half the recommended volume. We examined the quality of each library using a 4200 TapeStation and High Sensitivity D1000 ScreenTapes (Agilent Technologies, Santa Clara, CA, USA). Again, we quantified the amount of DNA with a Qubit fluorometer. Libraries were pooled so that they were equimolar and contained 20 to 25 individual libraries totaling 1 μg of DNA. These pools were hybridized using the myBaits Expert Predesigned Panel (Arbor Biosciences, Ann Arbor, MI, USA) Angiosperms353 v1 (Catalog #308196) (Johnson et al., 2019) following the manufacturer's protocol with v4 chemistry (http://www.arborbiosci.com/mybaits-manual). We hybridized libraries at 65°C for up to 32 h in a Hybex Microsample Incubator (Scigene, Sunnyvale, CA, USA). To prevent evaporation, we added an equal volume of red Chill-out Liquid Wax (Bio-Rad, Hercules, CA, USA) to each hybridization reaction.

We amplified the enriched products using the KAPA HiFi (2x) HotStart ReadyMix PCR Kit (Roche, Basel, Switzerland) for 10 cycles. PCR products were then cleaned using the QIAquick PCR purification kit (Qiagen, Manchester, UK). We performed another quantification with the Qubit fluorometer and, if necessary, re-amplified enriched products a second time for 3–8 cycles. We assessed quality and fragment size a final time using the TapeStation as above. Enriched library pools were then multiplexed and sequenced on an Illumina MiSeq (Illumina, San Diego, CA, USA) with v3 reagent chemistry (2 × 300-bp paired-end reads) at Royal Botanic Gardens, Kew, or on an Illumina HiSeq (2 × 150-bp paired-end reads) at Genewiz (Takeley, UK) or at Macrogen (Geumcheon, Republic of Korea).

For GAP samples, dried plant tissue (20–30 mg) was ground using a TissueLyser II (Qiagen) with tungsten carbide beads for simultaneous disruption and homogenization of the sample, per the manufacturer's instructions. Genomic DNA was extracted using the DNeasy Plant mini kit (Qiagen) as per the manufacturer's instructions on a QIAcube Connect (Qiagen). DNA quantity and quality were assessed using 1% E-gel with Sybr Safe dye (ThermoFisher) and concentrations were assessed using Quantifluor dsDNA assay (Promega, Madison, WI, USA). DNA samples were fragmented enzymatically as part of the NEBNext Ultra II FS library preparation workflow. Libraries were prepared using the NEBNext Ultra II FS Library Prep Kit (New England Biolabs), following the manufacturer's instructions with inserts of approximately 350 bp. Capture pools were 12–16 plex. Pooled libraries were enriched using the Angiosperms353 probe kit (Johnson et al., 2019) by hybridizing at 65°C with the Arbor Biosciences myBaits Expert Plant Angiosperms353 v1 probe set with V5 chemistry (Cat. # 308108.v5) following the manufacturer's instructions. Sequencing was performed on a NovaSeq. 6000 (Illumina) at the Australian Genome Research Facility (Melbourne) with v1.5 chemistry and 150 bp paired-end reads.

Contig assembly, multisequence alignment and paralog detection

We used HybPiper (v1.2) (Johnson et al., 2016) with default settings to process the raw sequence data. Briefly, reads were mapped to targets using BWA (v0.7.5a) (Li and Durbin, 2009), and successfully mapped reads were assembled into contigs using SPAdes (v3.11.1) (Bankevich et al., 2012). Then, Exonerate (Slater and Birney, 2005) was used to align contigs to their associated target exon sequence. If contigs were found to be overlapping (Johnson et al., 2016), they were combined into "supercontigs" that contain both target (exon) and off-target (intron) sequence data. Exonerate was then run again so that off-target regions could be more accurately identified. Sequences from 1KP transcriptomes were retrieved as described by Baker et al. (2022) and added to the corresponding HybPiper output FASTAs before alignment. In brief, BLASTN (Camacho et al., 2009) was used to match sequences to the

Angiosperms353 target file, and the best match was selected, trimming the gene to the BLAST hit.

Multisequence alignments were generated using two methods: MAFFT (v7.305) (Katoh and Standley, 2013) using the "auto" option and MAGUS (Smirnov and Warnow, 2021) with default options. The former is a classical method that aligns using Fourier transforms and automatically selects the appropriate algorithm for each input FASTA. The latter is a recent divide-and-conquer approach that uses MAFFT to generate subset alignments which are then merged using graph clustering.

We cleaned and trimmed alignments with GBLOCKS (v0.91b) (Castresana, 2000) and trimAl (v1.2) (Capella-Gutiérrez et al., 2009). For GBLOCKS, we used the minimum ("-b2 = 0") or default (85%) values for the minimum number of sequences for a flank position and allowed all gap positions ("-b5 = a"). For trimAl, we explored three different options: "gappyout", "automated1", and "gapthreshold = 0.2" following Portik and Wiens (2021).

Potentially paralogous sequences were flagged by HybPiper. Flagged sequences were retrieved, and RAxML (v8.2.9) (Stamatakis, 2014) was used to generate a phylogenetic tree of flagged sequences for each locus. If there is true paralogy at a locus, flagged sequences would be expected to group by paralog, rather than by specimen. Phylogenetic trees were plotted, and the presence of this pattern was examined by eye. If sequences from at least four species were found to group by paralog, the locus was classified as paralogous. Any locus that contained large numbers of specimens with flagged sequences (i.e., >30) was removed, regardless of how different paralogs grouped, because this situation may indicate an issue with recovery or contig generation. If a locus was classified as paralogous, the entire locus was removed from the data set. Note that paralogs could only be detected using those specimens that were run through the HybPiper pipeline (i.e., not including those where recoveries were previously done, such as 1KP data).

Filtering

We performed two main filtering steps to minimize gene tree error and identify a reliable and high-quality data set for phylogenetic inference (Figure 3). First, we removed sequences at each locus in which <10% of the length of the exon was recovered, before the alignment step. We also examined the effect this type of filtering had on phylogenetic reconstruction by varying the minimum percentage length threshold. The lowest value was 10%, followed by 25% and 50% in the most extreme filtering.

Second, we chose a set of loci for phylogenetic inference depending on the proportion of specimens for which a given exon length threshold was achieved. For example, one analysis we ran used a set of loci for which at least 50% of the exon was recovered in at least 50% of specimens. Again, we varied these threshold values from 10% to 25%, 50% and 75%, in eight different combinations to examine their effect on support metrics and tree topology. We also iterated through the two threshold parameters to examine how they interact and how their variation changes the number of loci selected as reliable for phylogenetic inference. Again, all filtering steps and calculations only included those species for which the recoveries were done in this study (i.e., not the 1KP data).

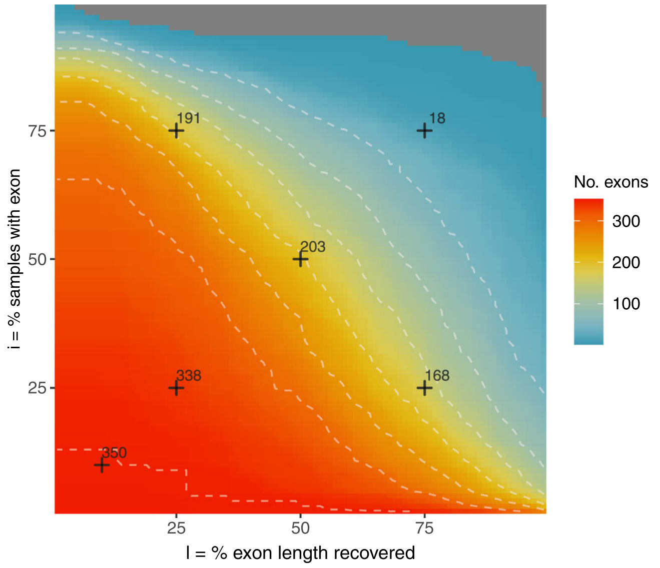

FIGURE 3 Heatmap of exon recovery. Each cell corresponds to the number of exons retained with different filtering thresholds. The *x*-axis is the minimum proportion of the exon length recovered (*l*), and the *y*-axis is the minimum proportion of samples (*i*) recovered. For example, for 191 exons, at least 25% of the length of the exon was recovered in 75% of samples. The dashed white lines are contours to show the slope of the surface. Crosses indicate the thresholds used to generate the range of trees assessed in this study.

Phylogenetic inference

We constructed phylogenetic trees using both coalescent and concatenation approaches, though our assessment of different methodological approaches was based on coalescent approaches for computational feasibility and ease of interpretation. The coalescent approach was implemented in ASTRAL-III (v5.7.7) (Zhang et al., 2018), which takes gene trees as input to construct a species tree and is particularly useful for incorporating gene tree discordance. Gene trees were constructed for each locus using RAxML (v8.2.9) (Stamatakis, 2014) using the rapid bootstrap "-f a" option with 100 bootstrap replicates to provide support values for downstream filtering. For each tree, we chose a GTRGAMMA model that uses empirical base frequencies, the gamma model of rate heterogeneity and the general time-reversible (GTR) matrix for substitution rates. Branches with bootstrap support <10% were collapsed using Newick Utilities program nw_ed (v1.6) (Junier and Zdobnov, 2010) to help improve the accuracy of downstream species tree inference. We then ran ASTRAL-III using the gene trees from our selected set of loci using options to output local posterior probability (LPP) "-t 3" and quartet support "-t 1".

The concatenation approach was implemented in IQ-TREE (v2.3.4) (Minh et al., 2020). After removing potential paralogs and filtering the data set, alignments were concatenated using the program phyx and its function pxcat (Brown et al., 2017). A separate substitution model was applied to each locus to account for rate variation. We ran IQTREE with the options "-m MFP + MERGE" to select the best partitioning scheme and associated models of molecular evolution for our data set with PartitionFinder (Lanfear et al., 2017) and the option "-bb 1000" to perform 1000 ultrafast bootstraps.

We used DiscoVista (Sayyari et al., 2018), a method to examine gene-tree incongruence, to examine how well species trees built with different sets of loci and different alignment/trimming methods supported major clades in magnoliids. We then examined gene tree conflict in detail for two contentious relationships in our trees, the placement of Hydnoraceae in Piperales and of the genus *Meiocarpidium* in Annonaceae. In addition, we calculated pairwise phylogenetic (Robinson-Foulds) distances among our different trees using the R package treedist (Smith, 2022).

We used four different summary statistics to evaluate the effect of using different approaches: (1) normalized scores output for each ASTRAL run that represent the percentage of gene trees that support the species tree; (2) the total number of quartets used in each analysis; (3) the mean local posterior probability (LPP) across the tree; and (4) the mean quartet support (QS), i.e., the proportion of quartets that support the branch in the species tree, averaged across the tree.

RESULTS AND DISCUSSION

Performance of Angiosperms353 in magnoliids

The average length of exon recovered was 393 bp (SD: 286 bp), which increased slightly after alignment (mean: 479 bp, SD: 307 bp) and even more after we added and aligned intronic data (mean: 730 bp, SD: 428 bp). The distributions of each of these lengths are visualized as density plots in Appendix S2. A total of nine putatively paralogous loci were detected and removed from all downstream analyses. In general, the kit performed reasonably well across most magnoliid orders, given the vast taxonomic scope of our study. We found that just over 50 loci were consistently well recovered across the different orders (Appendix S3). This low number is likely because the performance of the kit, and the different loci within the kit, varied among different taxonomic groups. Angiosperms353 performed well in groups such as Annonaceae, Monimiaceae, and Canellales, but we found that recoveries were generally poor throughout other families such as Lauraceae and Myristicaceae, similar to what was observed by Frost et al. (2022). We also found that relatively few high-quality loci were recovered in Piperales (Table 1), and many of these did not overlap with those in the other orders (Appendix S3). It may be that bait kits specific to these groups would help improve recoveries, though it may also be that some groups are more difficult to sequence (e.g., because of secondary compounds inhibiting recovery success) than others. For example, Annonaceae performed very well using both general (Appendix S4) and specific bait kits (Couvreur et al., 2019; Fonseca et al., 2024) while Myristicaceae has been consistently difficult to sequence using Angiosperms353 (Frost et al., 2022). In general, we found that the bait kit yielded higher support values toward the tips of the tree (node depth <5) than toward the root (Appendix S5), but the differences were not substantial.

TABLE 1 Numbers of exons selected as suitable for phylogenetic analyses per order. Each column indicates a different filtering threshold relating to the proportion of exon recovered (*l*) and the percentage of individuals achieving this proportion (*i*).

Order	*l* = 10%, *i* = 10%	*l* = 25%, *i* = 25%	*l* = 50%, *i* = 50%	*l* = 75%, *i* = 75%
Canellales	349	339	225	60
Chloranthales	341	334	210	31
Laurales	348	331	148	7
Magnoliales	349	332	231	54
Piperales	335	279	78	0

We built a range of phylogenetic trees using 16 to 341 loci from the Angiosperms353 kit. In general, coalescent (using ASTRAL) and concatenation (using IQTREE) approaches yielded similar topologies (Figure 5; Appendices S6–S8). The few notable differences concentrated in Aristolochiaceae (most notably the placement of Hydnoraceae), Piperales, Lauraceae, Myristicaceae, and various subclades of Annonaceae (Appendix S8). These differences, particularly in Aristolochiaceae, Lauraceae, and Myristicaceae, could be attributed to the poor recoveries of specimens belonging to these clades (Appendix S4), rather than the tree inference approach. As a result, we reconstructed a phylogenetic tree without these specimens (those with <50 loci for which >50% of the exon length was recovered) to determine whether their removal influenced topology. We found that the effect of this treatment was relatively minor (Appendix S9), similar to the effect of changing methodological approaches (see below). The most notable change was that Hernandiaceae and Atherospermataceae swapped positions, likely due to a lack of other samples in this region (e.g., Siparunaceae). For the remainder of the results, we focus mostly on phylogenetic trees generated by ASTRAL because these allowed us to dive further into incongruence among different gene trees and differences in methodological approaches.

Effects of analytical choices on support metrics

We examined the effect of changing the stringency with which loci are filtered, sequences are aligned, and alignments are trimmed on tree topology and support. Loci were first filtered before alignment using a threshold *r* to remove sequences with only short fragments of exons, from 10 to 50% of the mean reference length. Increasing *r* tended to increase mean QS and reduce mean LPP (Appendix S10: Table S1). This pattern likely emerged because as *r* increased fewer quartets were available to evaluate species trees, but those that remained were based on more data and tended to be concordant with the species tree hypothesis.

Loci were then filtered based on whether a given proportion of the total length of exon was recovered (*l*) in a given proportion of the total number of individuals (*i*). We built a "locus surface" to demonstrate how changing these two filtering criteria altered the number of loci retained (Figure 3) and give an indication of the overall quality of our data set. When both locus filtering criteria were high ($l = 75\%$ and $i = 75\%$; the top right of Figure 3), most of the loci were removed from the data set, leaving just 18 to build the tree (before paralog removal). Decreasing the threshold on the proportion of individuals while maintaining large portions of the exons ($l = 75\%$ and $i = 25\%$; bottom right of Figure 3) substantially increased the number of loci to 168. Similarly, allowing for smaller portions of the exon to be used if they were present in the majority of individuals ($l = 25\%$ and $i = 75\%$, top left of Figure 3) led to 191 loci retained. Less-stringent filtering thresholds for both criteria ($l = 25\%$ and $i = 25\%$ to $l = 10\%$ and $i = 10\%$, bottom left of Figure 3) led to the highest locus retention (338 and 350, respectively). The center of the space ($l = 50\%$ and $i = 50\%$) yielded 203 loci. If strict filtering (i.e., $l = 75\%$ and $i = 75\%$) was used there were not enough independent loci to have high confidence in the species tree topology, which resulted in a substantially lower mean LPP and higher QS when compared to other filtering thresholds (Appendix S10: Table S2), similar to when we increased *r* (Appendix S10: Table S1). As filtering was relaxed and increasing numbers of loci were used, the pattern reversed—the large number of loci used meant that LPP was high as confidence in the species tree topology increased but more conflict was also introduced, which lowered QS. Quartet scores were lowest (~63%) in analyses where filtering was most relaxed ($l = 25\%$ and $i = 25\%$ or $l = 10\%$ and $i = 10\%$). We found that decreasing *l* and *i* seemed to have a greater effect on the number of loci kept in Piperales and Laurales when compared to the other orders (Table 1).

We used two aligners—MAFFT and MAGUS, but these tended to have relatively small effects on support metrics (Appendix S10: Table S3). When only exons were used (instead of supercontigs), trees had lower support scores (Appendix S10: Table S4). Modifying the approach to alignment trimming (Appendix S10: Table S5) revealed that methods that were less conservative (i.e., a higher amount of less-well aligned data was kept, leading to more quartets) generally resulted in higher LPP and QS. Across all analyses, average LPP ranged from 0.84 to 0.92 (mean = 0.89, SD = 0.02), QS varied from 62.52 to 70.19 (mean = 64.8%, SD = 2.1%) and normalized scores from 0.928 to 0.953 (mean = 0.948, SD = 0.006), indicating that in general, changing the methodological approach did not have a large effect on these support metrics. However, we found that the number of quartets used varied more than 10-fold, from approximately 1.62e + 9 to 2.06e + 10 (mean = 1.41e + 10, SD = 4.88e + 9). When examining the distribution of support within the trees, we found that uncertainty was generally concentrated in a few areas of the tree, regardless of the approach taken to build the tree. Poor support was most commonly found in Miliuseae (Annonaceae) and to a lesser extent in Mollinedioideae (Monimiaceae), Laureae (Lauraceae), and Myristicaceae (Figure 5). This uncertainty may be, at least in part, due to poor recoveries for some of the species sampled in these clades (Appendix S4).

Effects of analytical choices on tree topology

While we observed that support values varied little, analytical choices may still influence tree topology. We used DiscoVista to visualize how species trees built with different combinations of the filtering criteria, aligners, and trimmers outlined above affect the support for magnoliid families and orders (Appendix S11). Note that trees were evaluated after removal of the five taxa that tended to be in different positions in the different analyses (*Yasunia sessiliflora*, *Pleurothyrium trianae*, *Chlorocardium venenosum*, *Apollonias arnottii*, and *Potameia thouarsii*). Most of these clades were strongly supported in most cases. Exceptions included Aristolochiaceae, for which most analyses rejected monophyly of the family, likely due to the placement of Hydnoraceae relative to the other species (Figure 5; Appendix S11). Indeed, our IQTREE analysis provided strong support for the monophyly of Aristolochiaceae, with Hydnoraceae nested within (Appendix S7). There was also some uncertainty in Calycanthaceae as support was generally lower and rejected in a few cases (Appendix S11).

These results were generally mirrored when looking at the proportion of gene trees that supported major clades (Appendix S12) in our reference ASTRAL tree. Lauraceae had the highest number of gene trees that strongly rejected the monophyly of the family, though this was only roughly a quarter of the total number. For some small families (Siparunaceae and Calycanthaceae), the majority of loci could not be used to measure support because recoveries were poor. Similarly, few loci were available for Magnoliales, likely because most loci were not present in all of the numerous and highly divergent species required to validate this relationship.

To quantify how different analytical scenarios affect tree topology, we calculated pairwise Robinson-Foulds (RF) distances among our trees (Appendix S13). Distances appeared to be primarily dictated by how strict filtering with *r*, *l* and *i* was, with particularly high thresholds leading to very different tree topologies. These variables affect the amount of sequence data used to build a tree. In the most extreme cases, they lead to individual or locus dropout, which likely contributes significantly to the calculation of tree distances. Furthermore, extreme filtering resulted in many branches that were reconstructed using just a handful of loci, which can bias relationships if these happen to not match the true species tree.

When we examined our trees more closely, we found that differences in topology were consistently located in Myristicaceae, Miliuseae (Annonaceae) and Lauraceae, which were also generally the parts of the trees with low support. When *r* was at its highest ($r = 50\%$), major clades within Piperales were unstable or polyphyletic. When alignment trimmers and *r* were changed, the placement of families Atherospermataceae, Hernandiaceae, and Siparunaceae also varied in some cases. Despite these differences, we note that the majority of relationships remained stable despite methodological changes, suggesting that, with enough data, the analytical methods chosen should not change the downstream relationships significantly.

Choosing a reference species tree

The utility of a phylogenetic tree depends on the goals of the analysis. For example, one way would be to determine which one provides the strongest support for the major clades in the group of interest (here, magnoliid families and orders), in which case, we could choose a tree based on exons because support for major clades in this tree was among the highest (Appendix S11).

Alternatively, the metrics quantifying the level of support across all branches of the tree can be used to assess the robustness of the relationships in the tree and our confidence that they represent the species tree. However, this approach was made more complex because we found that different evaluation metrics were maximized with different analytical scenarios. The number of quartets was highest when filtering and trimming was less severe. This metric appeared to have weak, negative relationships (Appendix S14) with normalized scores (the proportion of gene tree quartets that match the species tree) and mean QS (i.e., these metrics were higher when fewer quartets were used). Scores and mean quartet support were maximized when *l* and *i* filtering was most stringent. Mean LPP was positively correlated with number of quartets and was maximized when trimming was done with relaxed trimming approaches (GBLOCKS, "–b2 = 0"; trimAl, "–gapthreshold=0.2"). We note that high support does not guarantee that the relationship reflects the true species tree, particularly when only a handful of loci are available to reconstruct a relationship. However, given that the majority of branches in most of our trees are supported by many well-recovered loci with independent histories, this type of bias is probably limited to parts of the tree with poor recoveries.

Overall, our results indicate that no single approach maximized all support metrics, but instead we found that several different approaches maximized different aspects, albeit with relatively limited effect on support and topology. To choose a single tree to represent relationships among magnoliid species, we first centered and scaled each metric by subtracting the mean and dividing by the standard deviation because the metrics were on very different scales and the standardization allowed us to sum the four metrics to give a score to each tree. We found that the tree presented in Figures 4 and 5 (mafft, gblocks option "–b2 0", r10, i50, l50) had the highest sum of the four scaled metrics (Appendix S10), so here we use this tree as the reference tree. However, we reiterate that some uncertainty remains about topology linked to methodological choices, as noted above. As a result, all remaining trees are provided at https://github.com/ajhelmstetter/magnoliids/tree/master/figures/astral_trees.

One take-home message from our analysis is to avoid extreme filtering in terms of removing loci or sequences, which can have a large effect on species relationships in the tree, particularly when data quality varies substantially across the data set. Extreme filtering in this case can cause large numbers of samples and/or loci to drop out, meaning that relationships are based off a vastly reduced set loci and/or taxa. However, we note that our work represents a single case study, and we encourage other researchers to explore the effect of varying parameters and using different programs to identify how these choices might affect their own results.

Magnoliid backbone

Our results lend further support to the split of magnoliids into two main clades: Canellales and Piperales, and Laurales and Magnoliales (Figure 4). Furthermore, the four orders and all 18 families sensu APG IV (2016) were recovered as monophyletic across all our analyses, except for Aristolochiaceae and in a few cases, Calycanthaceae (see below; Figure 5; Appendices S7, S11). These relationships emerged early in angiosperm molecular phylogenetics based on Sanger sequencing data and have remained stable ever since (Qiu et al., 1999; Sauquet et al., 2003; Soltis et al., 2011; Massoni et al., 2014). They were also confirmed by early and more recent phylogenomic studies based on plastid genomes (Moore et al., 2007; Li et al., 2019, 2021) and nuclear transcriptome data (Wickett et al., 2014; One Thousand Plant Transcriptomes Initiative, 2019). To the best of our knowledge, our study and the broader angiosperm-wide study by Zuntini et al. (2024) represent the first attempts to comprehensively sample all families of magnoliids (and most genera) in a phylogenomic framework based on nuclear genome data.

Our results are very similar to those of Zuntini et al. (2024) for magnoliids, based on the same nuclear data generated from the PAFTOL and GAP projects. However, our study differs in sampling more taxa (235 species and 199 genera vs. 223 species and 190 genera) and more comprehensive phylogenetic analyses. The latter were made possible by the smaller overall data set, thus providing a unique opportunity to explore and discuss the impact of nuclear genomic data on magnoliid phylogenetic relationships and classification.

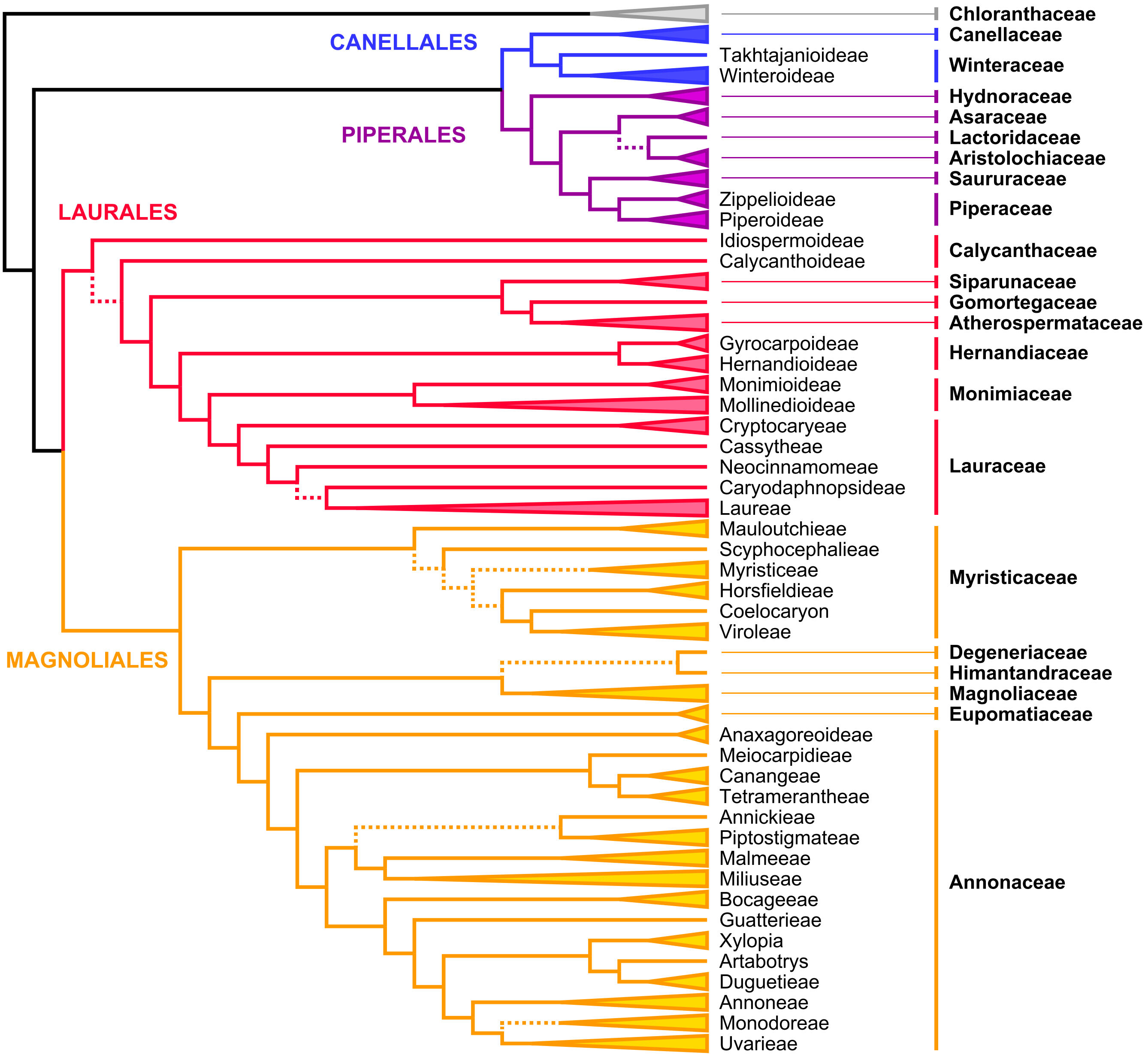

FIGURE 4 Summary of phylogenetic relationships in magnoliids obtained in the coalescent analysis of Angiosperms353 nuclear data. Triangles represent collapsed clades (for full detail, see Figure 5). Tip and clade labels correspond to the updated phylogenetic classification of magnoliids presented in this paper. Dashed branches received local posterior probabilities <0.95 in this analysis.

Within orders, our results broadly corroborate the relationships among families identified by previous studies, but also suggest potential solutions to long-term conflicts. In Piperales, our data suggest a new placement for the holoparasitic Hydnoraceae, with implications for the phylogenetic classification of the order. Indeed, a key question remains regarding the relationships among the traditional Aristolochiaceae, Lactoridaceae, and Hydnoraceae sensu APG III and previous classifications (APG III, 2009). Previous work had suggested that both Lactoridaceae and Hydnoraceae are nested in Aristolochiaceae (Naumann et al., 2013; Massoni et al., 2014), leading to the merging of the three families into a broader Aristolochiaceae (APG IV, 2016). However, a recent study based on data from all three plant genomes proposed recognizing instead four families (Aristolochiaceae, Asaraceae, Lactoridaceae, and Hydnoraceae) to account for both the high uncertainty persisting regarding their relationships and the strong morphological differentiation among these four clades (Figure 1C–G; Jost et al., 2021). Our coalescent analyses suggest that Hydnoraceae may be the sister group to all remaining Piperales, as also found by Zuntini et al. (2024). The most frequent topology (49%) in the gene trees used to build our reference tree (Figure 5) supported Hydnoraceae

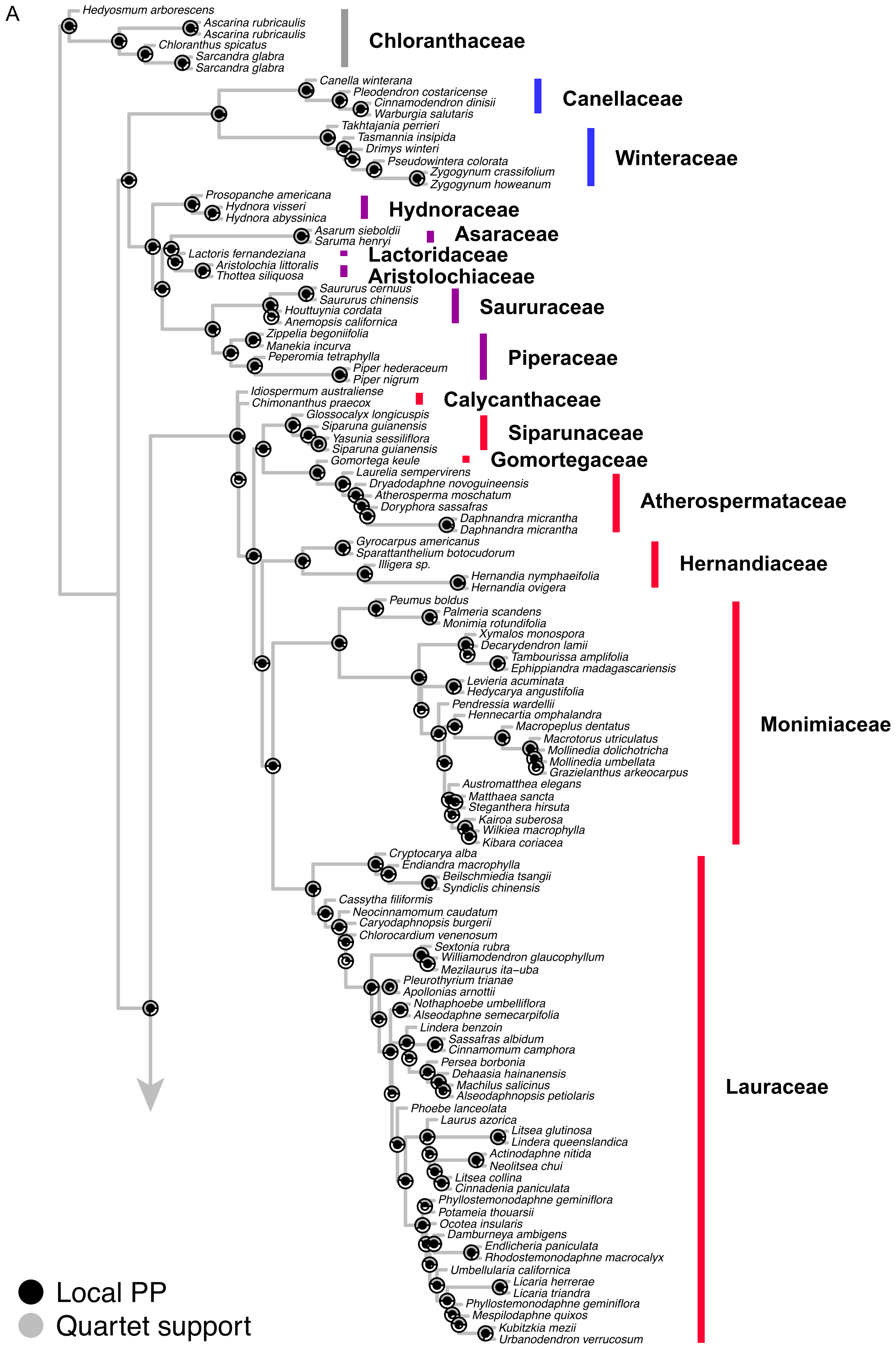

FIGURE 5 Phylogenetic relationships in magnoliids obtained in our main coalescent analysis (same tree as Fig. 4; also provided in high resolution in Appendix S6). This tree was reconstructed using the following methods: aligned with MAFFT, trimmed with gblocks option "–b2 = 0", and filtering thresholds of $r = 10\%$, $l = 50\%$ and $i = 50\%$. This tree achieved the highest combined support score of those compared (Appendix S10). At each node, the larger grey circle indicates quartet support (QS), and the inner black circle represents local posterior probability (local PP) for the subtending branch. Note that branch lengths are in coalescent units.

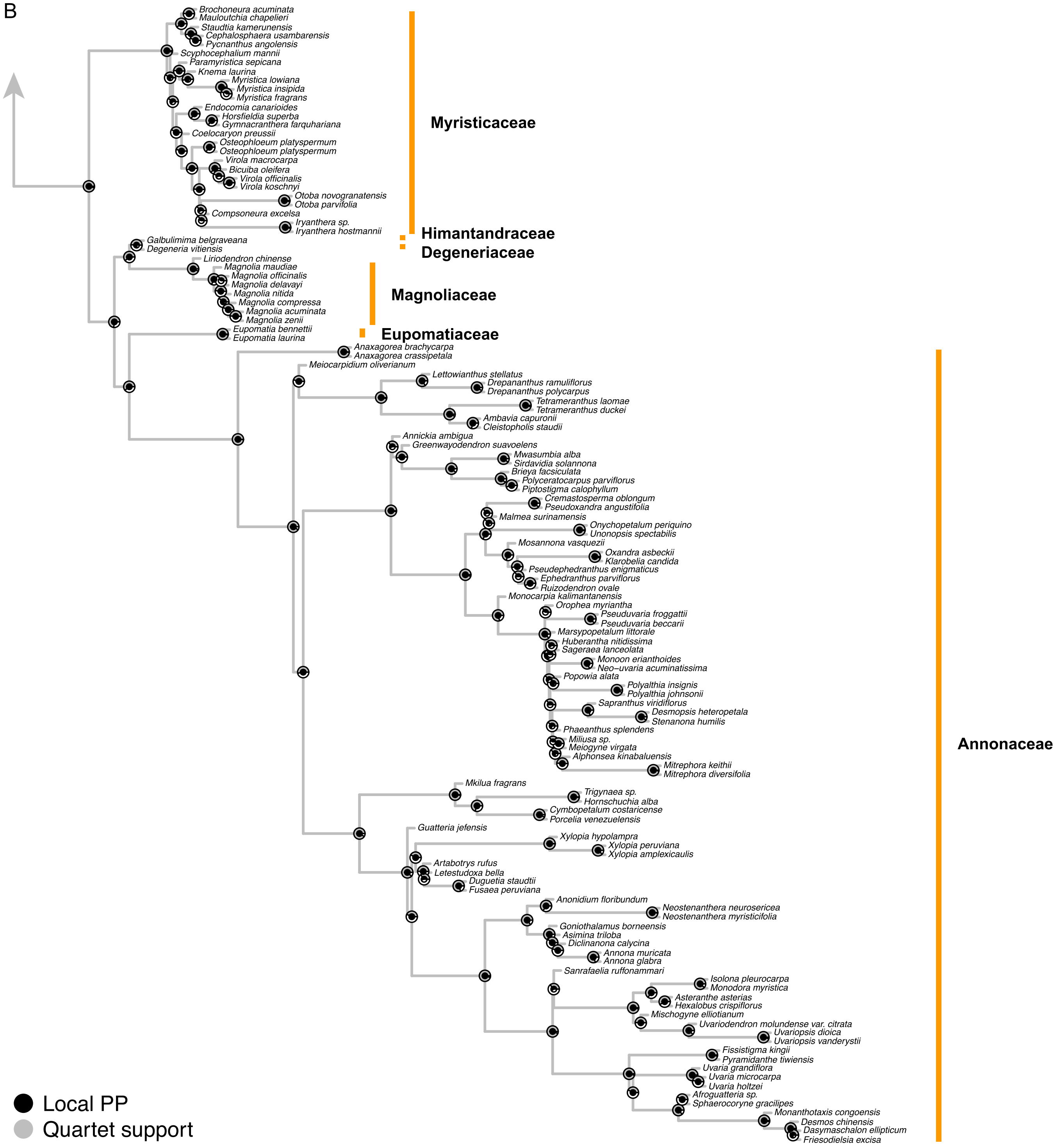

FIGURE 5 (Continued)

(*Hydnora* and *Prosopanche*) being distinct from other Aristolochiaceae sensu APG IV (Figure 6A). In contrast, our concatenation analysis (and a few coalescent ones) suggests a position nested in Aristolochiaceae sensu APG IV (Appendix S7), consistent with the main (137-loci) analysis of Jost et al. (2021). This alternative placement was also the second most frequent (36%) topology in our main coalescent analysis (Figure 6A), indicating that substantial conflict exists, even if the species tree topology is well-supported.

In Laurales, our results highlight conflicting relationships among Hernandiaceae, Lauraceae, and Monimiaceae, consistent with previous studies (Doyle and Endress, 2000; Renner and Chanderbali, 2000; Massoni et al., 2014). Both our

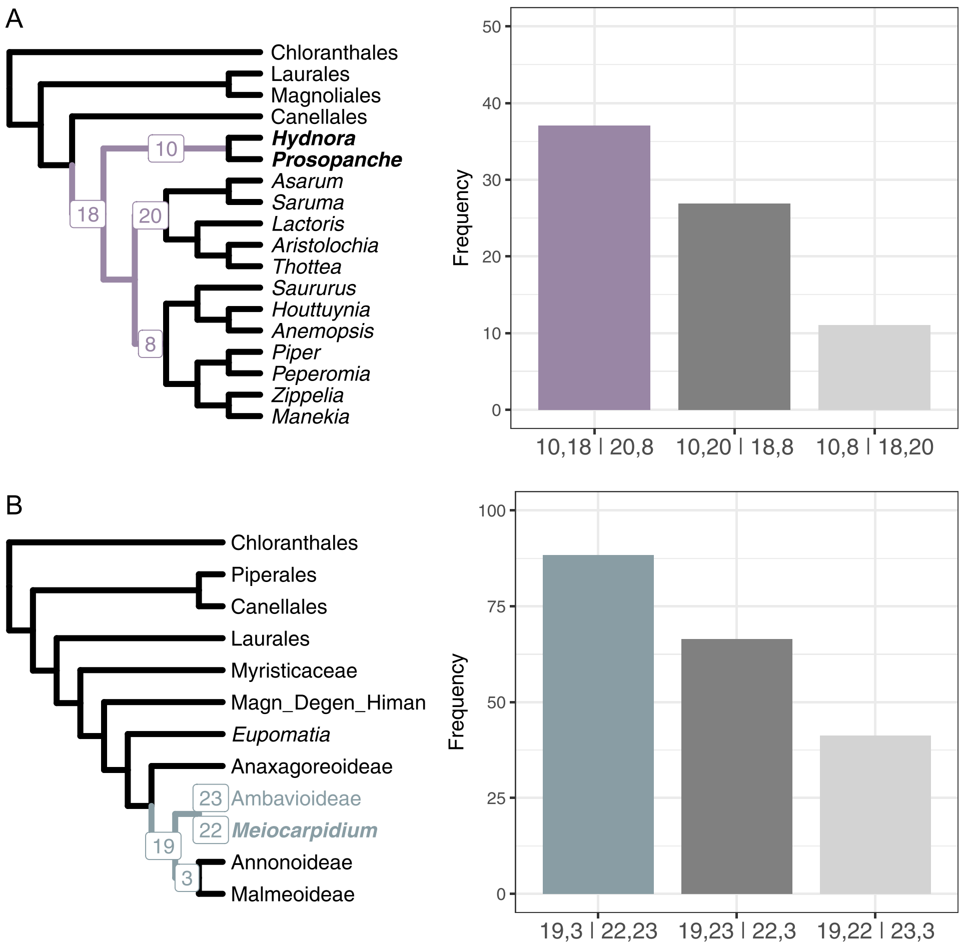

FIGURE 6 Topology tests to understand gene tree conflict for the placement of (A) Hydnoraceae and (B) *Meiocarpidium*. The left side is a summary tree with relevant branches colored and focal taxa bolded. Branch labels correspond to those used in the *x*-axis labels in the bar plots on the right. The bar plots show the frequency of each quartet, labelled below the bar. For the tree in (B), we combined Magnoliaceae, Himantandraceae and Degeneriaceae into a single tip.

coalescent and concatenation analyses suggest Hernandiaceae as the sister group to a clade comprising Lauraceae and Monimiaceae, as also found by Zuntini et al. (2024). In contrast, the majority of previous studies found Lauraceae to be sister to a clade including Hernandiaceae and Monimiaceae (Qiu et al., 1999; Soltis et al., 2011; One Thousand Plant Transcriptomes Initiative, 2019; Li et al., 2019, 2021). And conversely, analyses of morphological data strongly favored Monimiaceae as sister to a clade of Hernandiaceae and Lauraceae (Sauquet et al., 2003; Doyle and Endress, 2000, 2010). However, despite the apparent support for this relationship in the analyses presented here, these results should be taken with caution because it remained unstable across different analytical approaches. For instance, while all but two sensitivity analyses recovered Lauraceae and Monimiaceae as sister taxa, quartet support for this relationship remained weak across all analyses.

In Magnoliales, our data provide additional support for the placement of Magnoliaceae as sister to a clade of Degeneriaceae and Himantandraceae (Figure 5; Appendix S7), as also found by Zuntini et al. (2024). Previous studies that sampled the three families had either suggested the same arrangement with low support (reviewed by Massoni et al., 2014) or left these relationships unresolved (Qiu et al., 1999; Soltis et al., 2011; Massoni et al., 2014; Li et al., 2021), while combined analyses of molecular and morphological data had supported instead Magnoliaceae to be sister to a broader clade of Degeneriaceae, Himantandraceae, Eupomatiaceae, and Annonaceae (Doyle and Endress, 2000; Sauquet et al., 2003).

Relationships within families

Monimiaceae

The phylogenetic tree recovered two subfamilies for Monimiaceae, Monimioideae and Mollinedioideae, both with high support (Figure 5; Appendix S7). Renner et al. (2010) also recovered the same topology based on two cpDNA and one rDNA regions, as did Massoni et al. (2014) with six cpDNA regions, four mDNA, and two rDNA regions. *Hortonia*, the only genus of subfamily Hortonioideae, was initially sampled but resulted in low quality data and had to be excluded from our analyses. The genus was sampled in previous studies and was recovered as sister to Mollinedioideae with high support (Renner et al., 2010; Massoni et al., 2014). Relationships among the three genera of Monimioideae are consistent with previous work (Renner et al., 2010; Massoni et al., 2014), with *Peumus* sister to a clade comprising *Monimia* and *Palmeria*.

In Mollinedioideae, tribe Hedycaryeae was recovered as paraphyletic with *Xymalos*, *Decarydendron*, *Tambourissa*, and *Ephippiandra* as sister to a clade including *Hedycarya*, *Levieria* and other Mollinedioideae genera, however, with low support and unstable across our analyses (Figure 5; Appendix S7). Massoni et al. (2014) also recovered *Xymalos* in a clade with *Decarydendron* and *Tambourissa*. Instead, Renner et al. (2010) had found *Xymalos* as sister to all other Mollinedioideae genera. The presence of persistent tepals and fruiting receptacle not enclosing the drupelets support our findings positioning this genus as closely related to *Decarydendron* and *Tambourissa*.

The sister group to *Hedycarya* and *Levieria* includes all the genera assigned by Philipson (1987, 1988, 1993) to tribes Mollinedieae and Hennecartieae (with only the genus *Hennecartia*). Mollinedieae was recovered as paraphyletic due to the presence of Hennecartieae as the sister group of the neotropical Mollinedioideae clade. The circumscription of Hennecartieae relied on its discoid staminate flowers, anthers dehiscent by an equatorial slit, and pistillate flowers urceolate with oblate tepals (Philipson, 1988, 1993). Despite its peculiar morphology, *Hennecartia* was also recovered as sister to the other neotropical Mollinedieae genera by Renner et al. (2010), but it appeared as a sister group of *Wilkiea* from Australia and Southeast Asia in the analysis of Massoni et al. (2014). The enigmatic genera *Grazielanthus* and *Macrotorus* were placed in a clade with the remaining neotropical Mollinedieae genera, as reported by Renner et al. (2010). Mollinedieae was circumscribed by anthers with longitudinal slits, a pistillate receptacle opening by abscission of the upper part, and fruits exposed and attached to a reflexed fruiting receptacle enlarged. The genus *Macrotorus* was considered by Philipson (1987, 1988, 1993) as not sufficiently known to be placed because, at the time, only staminate flowers were known. The placement of *Macrotorus* in tribe Mollinedieae was accepted by subsequent authors (Peixoto and Pereira-Moura, 2008; Lírio et al., 2015, 2020) based on its flower and fruit features. The monotypic genus *Grazielanthus* had not yet been described when Philipson (1987, 1988, 1993) revised the classification of Monimiaceae; however, it was considered by Peixoto and Pereira-Moura (2008) as a member of Mollinedieae despite its non-calyptrate flowers, because all the other characteristics of the genus supported this placement.

Lauraceae

Our analyses recovered the main tribes of Lauraceae recognized in previous work. Hypodaphnideae, represented by the monotypic genus *Hypodaphnis*, was not included in our analyses due to low-quality data recovered. Cryptocaryeae (including *Cryptocarya*, *Endiandra*, *Syndiclis*, and *Beilschmiedia*) was recovered with high support, as in previous studies (Rohwer, 2000; Chanderbali et al., 2001; Li et al., 2020; Song et al., 2020). This tribe appears as the sister group to all other Lauraceae genera. Three monogeneric tribes were recovered as successive sister lineages to the remaining Lauraceae genera: Cassytheae (*Cassytha*), Neocinnamomeae (*Neocinnamomum*), and Caryodaphnopsideae (*Caryodaphnopsis*). These results generally agree with previous work (Rohwer, 2000; Chanderbali et al., 2001; Song et al., 2020), except for the relative positions of Cassytheae and Neocinnamomeae obtained by Chanderbali et al. (2001).

Tribe Laureae (as circumscribed by Song et al. 2020) was recovered as monophyletic, but with low support (Figure 5; Appendix S7). The genera *Sextonia*, *Williamodendron*, and *Mezilaurus* formed a clade sister to a clade comprising the *Persea*-*Cinnamomum* group and other Cinnamomeae genera. The *Persea*-*Cinnamomum* lineage is sister to a clade including *Laurus*, *Neolitsea*, and allies and to the clade comprising *Damburneya*, *Licaria*, and allies. The genera *Apollonias*, *Chlorocardium*, *Phoebe*, and *Yasunia* appeared unstable in our trees.

Myristicaceae

Three previous studies have addressed phylogenetic relationships in Myristicaceae using mostly plastid markers sampled from 16, 14, and 15 genera, respectively (Sauquet et al., 2003; Massoni et al., 2014; Frost et al., 2022). While the most recent study provided the most densely sampled phylogenetic tree in terms of species (53; Frost et al., 2022), our new analyses, using nuclear markers sampled from 19 of 21 genera, allow for the first time the delimitation of five tribes based on clades recovered with high support.

A strongly supported clade of five Malagasy and African genera (i.e., *Brochoneura*, *Cephalosphaera*, *Mauloutchia*, *Pycnanthus*, and *Staudtia*) was found to be sister to the remainder of the family. All of these genera plus *Doyleanthus* (not sampled here) were previously recovered as a monophyletic group of two sister clades informally named the "pycnanthoids" and "mauloutchioids" (Sauquet et al., 2003; Massoni et al., 2014; Frost et al., 2022). This clade is formally described here as tribe Mauloutchieae (Appendix 1), including *Doyleanthus* based on previous work (Sauquet et al., 2003). Within this tribe, the Malagasy (*Brochoneura*, *Mauloutchia*) and African (*Cephalosphaera*, *Pycnanthus*, *Staudtia*) genera form two strongly supported clades, whereas the latter was previously recovered as a grade (Sauquet et al., 2003; Frost et al., 2022). Of all the tribes, Mauloutchieae exhibits by far the widest range of morphological diversity, particularly in anther types, fruit ornamentation, dehiscence, aril type, and endosperm rumination (Sauquet et al., 2003).

The Central African genus *Scyphocephalium* had not been sampled in any previous molecular work. It appears isolated as sister to a large clade consisting of all Asian and neotropical genera in our coalescent tree (Figure 5). Although the genus was resolved in a different position in our concatenation analysis (Appendix S7), namely, nested in the Mauloutchieae with *Paramyristica*, we treat this alternative position, for both taxa, as a likely reconstruction artifact. Due to its topological isolation along with its unique inflorescence morphology (Figure 2B), *Scyphocephalium* is here classified into a separate tribe, Scyphocephalieae.

The Asian genera were recovered in two well-supported clades, but with uncertain relationships. Previous studies based on mostly plastid markers (Sauquet et al., 2003; Massoni et al., 2014; Frost et al., 2022) had yielded somewhat different relationships; the most notable difference was the association of *Gymnacranthera* with *Knema* and *Myristica* rather than with *Horsfieldia* as in this new study. The two Asian clades are here recognized as separate tribes: Horsfieldieae and Myristiceae (Appendix 1). Generic relationships within Horsfieldieae are well supported as [*Endocomia* [*Gymnacranthera* + *Horsfieldia*]]. Myristiceae is represented by the sister pair of *Knema* and *Myristica*, along with the monotypic genus *Paramyristica* in our coalescent tree (Figure 5). Despite the alternative placement of this genus in the concatenation analysis (Appendix S7), we tentatively assign *Paramyristica* to Myristiceae.

Coelocaryon is isolated in all analyses and consistently appears as sister to Viroleae. However, its position is poorly supported and appears erratic. For example, when exon filtering in coalescent analyses is changed to 75%, it appears sister to Myristiceae with poor support. The well-supported sister relationship between *Coelocaryon* and *Pycnanthus* seen in prior plastid analyses (Sauquet et al., 2003; Massoni et al., 2014; Frost et al., 2022) was not recovered. Due to this conflict, we believe further data will be required before assigning *Coelocaryon* to any tribe.

All the neotropical genera formed a well-supported clade, here recognized as tribe Viroleae. Within this tribe, relationships remain largely unclear with no single topology well supported. The Brazilian endemic genus *Bicuiba*, originally described as a species of *Virola* and subsequently segregated as a monotypic genus by de Wilde (1991) on the basis of its inflorescence structure, appears to be nested in *Virola*. A recently published molecular study of *Otoba* resolved this genus as sister to the rest of the tribe, albeit with poor support (posterior probability <0.5) (Frost et al., 2022). In previous phylogenetic studies, *Otoba* was recovered in a clade with the African genera *Coelocaryon* and *Pycnanthus* (Sauquet et al., 2003; Massoni et al., 2014; but see below).

Haematodendron, a monotypic Malagasy genus, was not included in this study, and its placement is not yet resolved. Previously, it was recovered as sister to either *Bicuiba* (Sauquet et al., 2003) or *Staudtia* (Massoni et al., 2014), in both instances with poor support. However, preliminary analyses of GenBank sequences of this genus found it to be identical to newly generated sequences of *Otoba* (L. Lagomarsino, Louisiana State University, personal communication), suggesting these previous results might be explained by an error in labeling molecular data generated for these two genera in the original study by Sauquet et al. (2003). *Haematodendron* and other Malagasy genera of Mauloutchieae share similarities of the androecia, pollen, and aril, but differ in floral shape and endosperm ruminations (Kühn and Kubitzki, 1993). Therefore, until further information becomes available, *Haematodendron* remains incertae sedis at tribal level.

Annonaceae

The inferred phylogenetic relationships within Annonaceae are broadly similar to those inferred using an Annonaceae specific nuclear probe set (Couvreur et al., 2019) and plastid data (Chatrou et al., 2012; Guo et al., 2017). Small differences with these previous studies were mainly concentrated along short branches with low overall support, especially along the backbone of tribe Miliuseae. Interestingly, there is little overlap in terms of regions between the two probe kits, with only 12 Annonaceae loci overlapping with the Angiosperms353 kit. These observations suggest that the probe set of Couvreur et al. (2019) could be combined with the Angiosperms353 kit (Johnson et al., 2019) to increase resolution in certain tribes such as Miliuseae and Malmeeae. Such an approach has already been undertaken in families such as Brassicaceae (Hendriks et al., 2021).

We retrieved all four previously described subfamilies as monophyletic and well supported, namely, Anaxagoreoideae, Ambavioideae, Annonoideae, and Malmeoideae. Phylogenetic relationships among genera are largely consistent with previously published results (Chatrou et al., 2012; Guo et al., 2017; Couvreur et al., 2019), and therefore, we will address only cases that diverge from previous findings.

The central African monotypic genus *Meiocarpidium* was recovered as sister to the rest of Ambavioideae with good support (1.0 LPP). However, we found substantial gene tree conflict in this relationship (Figure 6B). The most frequent quartet topology (45%) was only slightly more common than the others (34%), but was supported by a large number of loci, resulting in high confidence in the species tree topology. *Meiocarpidium* was included in Ambavioideae in all but one of our filtering scenarios. Under the most stringent scenario ($l = 75\%$, $i = 75\%$), *Meiocarpidium* was recovered as sister to Annonoideae and Malmeoideae; however, as indicated above, this filter setting resulted in very few markers retained, and support for this relationship was relatively low.

The position of *Meiocarpidium* has been debated over the years with some authors suggesting it should be assigned to its own subfamily, Meiocarpidioideae (Chaowasku, 2020). This decision was based on a phylogenetic tree obtained from the analysis of eight plastid markers, which had reconstructed

Meiocarpidium as sister to the rest of Annonaceae excluding *Anaxagorea* with mixed support values (Chaowasku, 2020), thus rendering Ambavioideae paraphyletic. However, this result was never inferred in previous phylogenetic studies of the family also based on plastid markers. *Meiocarpidium* was always inferred as sister to the rest of the Ambavioideae with different levels of support from weak to strong (Chatrou et al., 2012; Guo et al., 2017; Couvreur et al., 2008, 2019). Given the results presented here and those based independently on the Annonaceae specific probes (Couvreur et al., 2019), we do not advocate the establishment of subfamily Meiocarpidioideae. Furthermore, adopting a subfamily view would not be consistent with other similar cases across the family. For instance, the genus *Annickia* was inferred as sister to the rest of Malmeoideae, but was recognized at tribe level (Annickieae), but not subfamily level (Couvreur et al., 2019). Thus, we propose that the monotypic genus *Meiocarpidium* instead be assigned to the new tribe Meiocarpidieae within Ambavioideae, in addition to the two that already exist (i.e., Tetramerantheae and Canangeae; see Appendix 1).

One surprising outcome of our nuclear phylogenetic analysis (Figure 5) compared to previous plastid phylogenetic studies is the non-monophyly of tribe Xylopieae also recovered using the Annonaceae kit (Couvreur et al., 2019). This tribe is composed of two genera: *Xylopia*, a pantropical genus of trees, and *Artabotrys*, a paleotropical genus of lianas. Plastid phylogenetic trees of Annonaceae have consistently inferred a strongly supported sister relationship between the two genera, both in family-level (one species per genus sampled) (Chatrou et al., 2012; Guo et al., 2017) and tribal-level (several species per genus) studies (Thomas et al., 2015). This result was confirmed in a separate, recent phylogenomic study of Annonaceae, resulting in the transfer of *Artabotrys* from Xylopieae to Duguetieae (Nge et al., 2024), which we follow here.

Finally, *Sanrafaelia* was inferred as sister to tribe Uvarieae, albeit with relatively low support, confirming the results of Couvreur et al. (2019), but in contrast with the results based on plastid markers (Chatrou et al., 2012; Guo et al., 2017; Couvreur et al., 2008, 2019). *Sanrafaelia* and its sister genus *Ophrypetalum* (not sampled here) were recently transferred to a new tribe based on a phylogenetic analysis of tribe Monodoreae using the Annonaceae probes (Dagallier et al., 2023).

PHYLOGENETIC CLASSIFICATION OF MAGNOLIIDS

Here we propose an updated phylogenetic classification for magnoliids (sensu APG IV, 2016; Magnoliidae sensu Cantino et al., 2007; Magnolianae sensu Chase and Reveal, 2009) consistent with the nuclear phylogenomic analyses presented here (Figure 4) and with recent phylogenetic studies using a variety of sequencing approaches in the larger families. In doing so, we aim at maximum stability by following recent phylogenetic classifications presented at the angiosperm level by the Angiosperm Phylogeny Group and at the family level by experts of these clades.

Briefly, we follow APG IV (2016) for orders and families, except for Aristolochiaceae for which we recognize four separate families following Jost et al. (2021). For Piperaceae, we follow Samain et al. (2008). For Hernandiaceae, we follow Michalak et al. (2010) in recognizing *Hazomalania* as a distinct genus. For Monimiaceae, we recognize the same three subfamilies as Philipson (1987, 1988, 1993), but none of the tribes at this stage as doing so would require additional sampling and resolution among genera of Mollinedioideae. For Lauraceae, we follow strictly Song et al. (2020) in recognizing six tribes. We acknowledge that, given the size of the family, it would seem more appropriate to recognize subclades at the subfamily level instead. However, we feel it would be premature to propose an alternative to the latest phylogenetic system published by experts of the family, given our limited sample of genera here. For Myristicaceae, we propose the first formal infrafamilial classification by describing five new tribes, based in part on the informal clade names introduced by Sauquet et al. (2003). Lastly, for Annonaceae, we follow the well-established system of subfamilies and tribes of Chatrou et al. (2012), with the addition of five new tribes introduced in more recent studies (Guo et al., 2017; Couvreur et al., 2019; Chaowasku, 2020; Dagallier et al., 2023) and Meiocarpidieae recognized here for the first time. The taxonomic treatment for the new tribes in Myristicaceae and Annonaceae is provided in Appendix 1. Taxa not sampled in this study are marked with an asterisk.

Order Canellales Cronquist
Family Canellaceae Martius
 Canella, *Cinnamodendron*, *Cinnamosma**, *Pleodendron*, *Warburgia*

Family Winteraceae Lindley
 Subfamily Takhtajanioideae Leroy
  Takhtajania
 Subfamily Winteroideae Arnott
  Drimys, *Pseudowintera*, *Tasmannia*, *Zygogynum*

Order Piperales Dumortier
Family Hydnoraceae C. Agardh
 Hydnora, *Prosopanche*

Family Asaraceae Ventenat
 Asarum, *Saruma*

Family Lactoridaceae Engler
 Lactoris

Family Aristolochiaceae Jussieu
 Aristolochia, *Thottea*

Family Saururaceae Richard
 Anemopsis, *Gymnotheca**, *Houttuynia*, *Saururus*

Family Piperaceae Giseke
- Subfamily Verhuellioideae* Samain & Wanke
  - *Verhuellia**
- Subfamily Zippelioideae Samain & Wanke
  - *Manekia*, *Zippelia*
- Subfamily Piperoideae Arnott
  - *Peperomia*, *Piper*

Order Laurales Berchtold & Presl
Family Calycanthaceae Lindley
- Subfamily Calycanthoideae Burnett
  - *Calycanthus*, *Chimonanthus*
- Subfamily Idiospermoideae Thorne
  - *Idiospermum*

Family Siparunaceae (A. DC.) Schodde
- *Glossocalyx*, *Siparuna*

Family Gomortegaceae Reiche
- *Gomortega*

Family Atherospermataceae R. Brown
- *Atherosperma*, *Daphnandra*, *Doryphora*, *Dryadodaphne*, *Laurelia*, *Laureliopsis**, *Nemuaron**

Family Hernandiaceae Blume
- Subfamily Gyrocarpoideae Pax
  - *Gyrocarpus*, *Sparattanthelium*
- Subfamily Hernandioideae
  - *Hazomalania**, *Hernandia*, *Illigera*

Family Monimiaceae Jussieu
- Subfamily Monimioideae Rafinesque
  - *Monimia*, *Palmeria*, *Peumus*
- Subfamily Hortonioideae* Thorne & Reveal
  - *Hortonia**
- Subfamily Mollinedioideae Thorne
  - *Austromatthaea*, *Decarydendron*, *Ephippiandra*, *Grazielanthus*, *Hedycarya*, *Hemmantia**, *Hennecartia*, *Kairoa*, *Kibara*, *Kibaropsis**, *Lauterbachia*, *Levieria*, *Macropeplus*, *Macrotorus*, *Matthaea*, *Mollinedia*, *Parakibara**, *Pendressia*, *Steganthera*, *Tambourissa*, *Wilkiea*, *Xymalos*

Family Lauraceae Jussieu
- Tribe Hypodaphnideae* Kosterm. ex Reveal
  - *Hypodaphnis**
- Tribe Cryptocaryeae Nees
  - *Aspidostemon**, *Beilschmiedia*, *Cryptocarya*, *Dahlgrenodendron**, *Endiandra**, *Eusideroxylon**, *Potameia**, *Potoxylon**, *Ravensara**, *Sinopora**, *Syndiclis*, *Triadodaphne**, *Yasunia*
- Tribe Cassytheae Dumortier
  - *Cassytha*
- Tribe Neocinnamomeae Yu Song, W.B. Yu & Y.H. Tan
  - *Neocinnamomum*
- Tribe Caryodaphnopsideae Yu Song, W.B. Yu & Y.H. Tan
  - *Caryodaphnopsis*
- Tribe Laureae Maout & Decaisne
  - *Actinodaphne*, *Adenodaphne**, *Aiouea*, *Alseodaphne*, *Alseodaphnopsis*, *Anaueria**, *Aniba**, *Apollonias*, *Chlorocardium*, *Cinnadenia*, *Cinnamomum*, *Clinostemon**, *Damburneya*, *Dehaasia*, *Dicypellium**, *Dodecadenia**, *Endlicheria*, *Iteadaphne**, *Kubitzkia*, *Laurus*, *Licaria*, *Lindera*, *Litsea*, *Machilus*, *Mespilodaphne*, *Mezilaurus*, *Mocinnodaphne**, *Nectandra**, *Neolitsea*, *Nothaphoebe*, *Ocotea**, *Paraia**, *Parasassafras**, *Persea*, *Phoebe*, *Phyllostemonodaphne*, *Pleurothyrium*, *Povedadaphne**, *Rhodostemonodaphne*, *Sassafras*, *Sextonia*, *Sinosassafras**, *Umbellularia*, *Urbanodendron*, *Williamodendron*

Order Magnoliales Bromhead
Family Myristicaceae R. Brown
- Tribe Mauloutchieae Ezedin & Sauquet, trib. nov.
  - *Brochoneura*, *Cephalosphaera*, *Doyleanthus**, *Mauloutchia*, *Pycnanthus*, *Staudtia*
- Tribe Scyphocephalieae Ezedin & Sauquet, trib. nov.
  - *Scyphocephalium*
- Tribe Horsfieldieae Ezedin & Sauquet, trib. nov.
  - *Endocomia*, *Gymnacranthera*, *Horsfieldia*
- Tribe Myristiceae Ezedin & Sauquet, trib. nov.
  - *Knema*, *Myristica*, *Paramyristica*
- Tribe Viroleae S.M.Oliveira & Sauquet, trib. nov.
  - *Bicuiba*, *Compsoneura*, *Iryanthera*, *Osteophloeum*, *Otoba*, *Virola*
- Incertae sedis
  - *Coelocaryon*, *Haematodendron**

Family Degeneriaceae I.W. Bailey & A.C. Smith
- *Degeneria*

Family Himantandraceae Diels
- *Galbulimima*

Family Magnoliaceae Jussieu
- *Liriodendron*, *Magnolia*

Family Eupomatiaceae Orban
- *Eupomatia*

Family Annonaceae Jussieu
- Subfamily Anaxagoreoideae Chatrou, Pirie, Erkens & Couvreur
  - *Anaxagorea*
- Subfamily Ambavioideae Chatrou, Pirie, Erkens & Couvreur
  - Tribe Meiocarpidieae Chatrou, Couvreur & Erkens, trib. nov.
    - *Meiocarpidium*
  - Tribe Canangeae Chaowasku
    - *Cananga**, *Cyathocalyx**, *Drepananthus*, *Lettowianthus*

Tribe Tetramerantheae R.E. Fr. ex Reveal
Ambavia, *Cleistopholis*, *Mezzettia**, *Tetrameranthus*
Subfamily Annonoideae Raf.
Tribe Bocageeae Endl.
*Bocagea**, *Cardiopetalum**, *Cymbopetalum*, *Froesiodendron**, *Hornschuchia*, *Mkilua*, *Porcelia*, *Trigynaea*
Tribe Guatterieae Hook.f. & Thomson
Guatteria
Tribe Xylopieae Endl.
Xylopia
Tribe Duguetieae Chatrou & R.M.K. Saunders
Artabotrys, *Duckeanthus**, *Duguetia*, *Fusaea*, *Letestudoxa*, *Pseudartabotrys**
Tribe Annoneae Endl.
Annona, *Anonidium*, *Asimina*, *Diclinanona*, *Disepalum**, *Goniothalamus*, *Neostenanthera*
Tribe Ophrypetaleae Dagallier & Couvreur
Ophrypetalum, Sanrafaelia*
Tribe Monodoreae Baill.
Asteranthe, Dennettia, Hexalobus, Isolona, Lukea*, Mischogyne, Monocyclanthus*, Monodora, Uvariastrum*, Uvariodendron, Uvariopsis*
Tribe Monodoreae Baill.
Asteranthe, *Dennettia**, *Hexalobus*, *Isolona*, *Lukea**, *Mischogyne*, *Monocyclanthus**, *Monodora*, *Ophrypetalum**, *Sanrafaelia*, *Uvariastrum**, *Uvariodendron*, *Uvariopsis*
Tribe Uvarieae Hook.f. & Thomson
Afroguatteria, *Cleistochlamys**, *Dasymaschalon*, *Desmos*, *Dielsiothamnus**, *Fissistigma*, *Friesodielsia*, *Monanthotaxis*, *Pyramidanthe*, *Sphaerocoryne*, *Toussaintia**, *Uvaria*
Subfamily Malmeoideae Chatrou, Pirie, Erkens & Couvreur
Tribe Annickieae Couvreur
Annickia
Tribe Piptostigmateae Chatrou & R.M.K. Saunders
Brieya, *Greenwayodendron*, *Mwasumbia*, *Piptostigma*, *Polyceratocarpus*, *Sirdavidia*
Tribe Malmeeae Chatrou & R.M.K. Saunders
*Bocageopsis**, *Cremastosperma*, *Ephedranthus*, *Klarobelia*, *Malmea*, *Mosannona*, *Onychopetalum*, *Oxandra*, *Pseudephedranthus*, *Pseudomalmea**, *Pseudoxandra*, *Ruizodendron*, *Unonopsis*
Tribe Maasieae* Chatrou & R.M.K. Saunders
*Maasia**
Tribe Fenerivieae* Chatrou & R.M.K. Saunders
*Fenerivia**
Tribe Phoenicantheae* X. Guo & R.M.K. Saunders
*Phoenicanthus**
Tribe Dendrokingstonieae* Chatrou & R.M.K. Saunders
*Dendrokingstonia**
Tribe Monocarpieae Chatrou & R.M.K. Saunders
*Leoheo**, *Monocarpia*
Tribe Miliuseae Hook.f. & Thomson
Alphonsea, *Desmopsis*, *Huberantha*, *Marsypopetalum*, *Meiogyne*, *Miliusa*, *Mitrephora*, *Monoon*, *Neo-uvaria*, *Orophea*, *Phaeanthus*, *Platymitra**, *Polyalthia*, *Polyalthiopsis**, *Popowia*, *Pseuduvaria*, *Sageraea*, *Sapranthus*, *Stelechocarpus**, *Stenanona*, *Tridimeris**, *Trivalvaria**, *Wangia**, *Winitia**, *Wuodendron**.

AUTHOR CONTRIBUTIONS

All authors jointly designed this study. Z.E., E.J.L., S.M.O., L.W.C., R.H.J.E., I.L., K.V., O.M., S.R., A.R.Z., W.J.B., T.L.P.C., F.F., and H.S. contributed data. A.J.H. performed all analyses. H.S. coordinated writing of the manuscript, with contributions from all authors.

AFFILIATIONS

[1]FRB-CESAB, Institut Bouisson Bertrand, 5 Rue de l'École de Médecine, Montpellier 34000, France

[2]ISEM, Univ. Montpellier, CNRS, IRD, Montpellier, France

[3]Department of Plant and Microbial Biology, University of Minnesota, Saint Paul, MN, USA

[4]Harvard University Herbaria, Cambridge, MA, USA

[5]Departamento de Botânica, Universidade de São Paulo, Rua do Matão 277, Edifício Sobre-as-ondas 05508-900, São Paulo, SP, Brazil

[6]Instituto Tecnológico Vale, Rua Boaventura da Silva, 955, Nazaré, Belém, PA 66055-090, Brazil

[7]Naturalis Biodiversity Center, Leiden 2333 CR, The Netherlands

[8]Systematic and Evolutionary Botany Lab, Department of Biology, Ghent University, Ghent, Belgium

[9]Maastricht Science Programme, Maastricht University, Maastricht, The Netherlands

[10]System Earth Science, Maastricht University, Venlo, The Netherlands

[11]Royal Botanic Gardens, Kew, Richmond, Surrey TW9 3AE, UK

[12]Meise Botanic Garden, Meise, Belgium

[13]Department of Biology, Aarhus University, Ny Munkegade 114-116, 8000 Aarhus C, Denmark

[14]IRD, DIADE, Univ Montpellier, Montpellier, France

[15]National Herbarium of NSW, Botanic Gardens of Sydney, Mount Annan, NSW, Australia

[16]Evolution and Ecology Research Centre, School of Biological, Earth and Environmental Sciences, University of New South Wales, Sydney, Australia

ACKNOWLEDGMENTS

We thank Associate Editor Jennifer Tate, Laura Lagomarsino, and an anonymous reviewer for comments that significantly improved this paper, Francis Nge for feedback on an earlier draft, and Theodore Allnutt for submission of GAP sequence data to the ENA. This work was funded by grants from the Calleva Foundation to the Plant and Fungal Trees of Life (PAFTOL) project at Royal Botanic Gardens, Kew. We acknowledge the contribution of the Genomics for Australian Plants Framework Initiative consortium (https://www.genomicsforaustralianplants.com/consortium/) in the generation of data used in this publication. The Initiative is supported by funding from Bioplatforms Australia (enabled by NCRIS), the Ian Potter Foundation, Royal Botanic Gardens Foundation (Victoria), Royal Botanic Gardens Victoria, the Royal Botanic

Gardens and Domain Trust, the Council of Heads of Australasian Herbaria, CSIRO, Centre for Australian National Biodiversity Research, and the Department of Biodiversity, Conservation and Attractions, Western Australia. Open access publishing facilitated by New South Wales Department of Planning and Environment, as part of the Wiley - New South Wales Department of Planning and Environment agreement via the Council of Australian University Librarians.

DATA AVAILABILITY STATEMENT

All new raw sequence data generated for this study have been deposited in the European Nucleotide Archive (see Appendix S1). Code, all phylogenetic trees, and additional associated data are available at Github: https://github.com/ajhelmstetter/PAFTOL_magnoliids.

ORCID

Andrew J. Helmstetter http://orcid.org/0000-0003-3761-4981
Elton John de Lírio http://orcid.org/0000-0002-9986-9640
Sylvia M. de Oliveira http://orcid.org/0000-0002-1440-9718
Lars W. Chatrou http://orcid.org/0000-0003-0131-0302
Roy H. J. Erkens http://orcid.org/0000-0002-1093-0370
Isabel Larridon http://orcid.org/0000-0003-0285-722X
Kevin Leempoel http://orcid.org/0000-0001-7335-7930
Olivier Maurin http://orcid.org/0000-0002-4151-6164
Shyamali Roy http://orcid.org/0000-0002-9129-2496
Alexandre R. Zuntini http://orcid.org/0000-0003-0705-8902
William J. Baker http://orcid.org/0000-0001-6727-1831
Thomas L. P. Couvreur http://orcid.org/0000-0002-8509-6587
Félix Forest http://orcid.org/0000-0002-2004-433X
Hervé Sauquet http://orcid.org/0000-0001-8305-3236

REFERENCES

APG. 1998. An ordinal classification for the families of flowering plants. *Annals of the Missouri Botanical Garden* 85: 531–553.

APG II. 2003. An update of the Angiosperm Phylogeny Group classification for the orders and families of flowering plants: APG II. *Botanical Journal of the Linnean Society* 141: 399–436.

APG III. 2009. An update of the Angiosperm Phylogeny Group classification for the orders and families of flowering plants: APG III. *Botanical Journal of the Linnean Society* 161: 105–121.

APG IV. 2016. An update of the Angiosperm Phylogeny Group classification for the orders and families of flowering plants: APG IV. *Botanical Journal of the Linnean Society* 181: 1–20.

Baker, W. J., P. Bailey, V. Barber, A. Barker, S. Bellot, D. Bishop, L. R. Botigué, et al. 2022. A comprehensive phylogenomic platform for exploring the angiosperm Tree of Life. *Systematic Biology* 71: 301–319.

Baker, W. J., S. Dodsworth, F. Forest, S. W. Graham, M. G. Johnson, A. McDonnell, L. Pokorny, et al. 2021. Exploring Angiosperms353: an open, community toolkit for collaborative phylogenomic research on flowering plants. *American Journal of Botany* 108: 1059–1065.

Bankevich, A., S. Nurk, D. Antipov, A. A. Gurevich, M. Dvorkin, A. S. Kulikov, V. M. Lesin, et al. 2012. SPAdes: a new genome assembly algorithm and its applications to single-cell sequencing. *Journal of Computational Biology* 19: 455–477.

Brown, J. W., J. F. Walker, and S. A. Smith. 2017. Phyx: phylogenetic tools for unix. *Bioinformatics* 33: 1886–1888.

Camacho, C., G. Coulouris, V. Avagyan, N. Ma, J. Papadopoulos, K. Bealer, and T. L. Madden. 2009. BLAST+: architecture and applications. *BMC Bioinformatics* 10: 421.

Cantino, P. D., J. A. Doyle, S. W. Graham, W. S. Judd, R. G. Olmstead, D. E. Soltis, P. S. Soltis, and M. J. Donoghue. 2007. Towards a phylogenetic nomenclature of *Tracheophyta*. *Taxon* 56: E1–E44.

Capella-Gutiérrez, S., J. M. Silla-Martínez, and T. Gabaldón. 2009. trimAl: a tool for automated alignment trimming in large-scale phylogenetic analyses. *Bioinformatics* 25: 1972–1973.

Castresana, J. 2000. Selection of conserved blocks from multiple alignments for their use in phylogenetic analysis. *Molecular Biology and Evolution* 17: 540–552.

Chanderbali, A. S., H. van der Werff, and S. S. Renner. 2001. Phylogeny and historical biogeography of Lauraceae: evidence from the chloroplast and nuclear genomes. *Annals of the Missouri Botanical Garden* 88: 104–134.

Chaowasku, T. 2020. Toward a phylogenetic reclassification of the subfamily Ambavioideae (Annonaceae): establishment of a new subfamily and a new tribe. *Acta Botanica Brasilica* 34: 522–529.

Chase, M. W., and J. L. Reveal. 2009. A phylogenetic classification of the land plants to accompany APG III. *Botanical Journal of the Linnean Society* 161: 122–127.

Chatrou, L. W., M. D. Pirie, R. H. J. Erkens, T. L. P. Couvreur, K. M. Neubig, J. R. Abbott, J. B. Mols, et al. 2012. A new subfamilial and tribal classification of the pantropical flowering plant family Annonaceae informed by molecular phylogenetics. *Botanical Journal of the Linnean Society* 169: 5–40.

Couvreur, T. L. P., A. J. Helmstetter, E. J. M. Koenen, K. Bethune, R. D. Brandão, S. A. Little, H. Sauquet, and R. H. J. Erkens. 2019. Phylogenomics of the major tropical plant family Annonaceae using targeted enrichment of nuclear genes. *Frontiers in Plant Science* 9: 1941.

Couvreur, T. L. P., J. E. Richardson, M. S. M. Sosef, R. H. J. Erkens, and L. W. Chatrou. 2008. Evolution of syncarpy and other morphological characters in African Annonaceae: A posterior mapping approach. *Molecular Phylogenetics and Evolution* 47: 302–318.

Cronquist, A. 1981. An integrated system of classification of flowering plants. Columbia University Press, NY, NY, USA.

Dagallier, L.-P. M. J., F. M. Mbago, M. Couderc, M. Gaudeul, A. Grall, C. Loup, J. J. Wieringa, et al. 2023. Phylogenomic inference of the African tribe Monodoreae (Annonaceae) and taxonomic revision of *Dennettia*, *Uvariodendron* and *Uvariopsis*. *PhytoKeys* 233: 1–200.

de Wilde, W. J. J. O. 1984. *Endocomia*, a new genus of Myristicaceae. *Blumea* 30: 173–196.

de Wilde, W. J. J. O. 1991. The genera of Myristicaceae as distinguished by their inflorescences, and the description of a new genus, *Bicuiba*. *Beiträge zur Biologie der Pflanzen* 66: 95–125.

de Wilde, W. J. J. O. 1994. *Paramyristica*, a new genus of Myristicaceae. *Blumea* 39: 341–350.

Doyle, J. J., and J. L. Doyle. 1987. A rapid DNA isolation procedure for small quantities of fresh leaf tissue. *Phytochemical Bulletin* 19: 11–15.

Doyle, J. A., and P. K. Endress. 2000. Morphological phylogenetic analysis of basal angiosperms: comparison and combination with molecular data. *International Journal of Plant Sciences* 161: S121–S153.

Doyle, J. A., and P. K. Endress. 2010. Integrating Early Cretaceous fossils into the phylogeny of living angiosperms: Magnoliidae and eudicots. *Journal of Systematics and Evolution* 48: 1–35.

Endress, P. K. 1987. The early evolution of the angiosperm flower. *Trends in Ecology & Evolution* 2: 300–304.

Endress, P. K., and J. A. Doyle. 2009. Reconstructing the ancestral angiosperm flower and its initial specializations. *American Journal of Botany* 96: 22–66.

Endress, P. K., and J. A. Doyle. 2015. Ancestral traits and specializations in the flowers of the basal grade of living angiosperms. *Taxon* 64: 1093–1116.

Ezedin, Z., and H. Sauquet. 2024. (3021–3022) Proposals to conserve the names *Brochoneura*, with a conserved type, and *Cephalosphaera* (Myristicaceae). *Taxon* 73: 648–649.

Figueiredo, E., and G. F. Smith. 2020. Nomenclature of *Brochoneura* and *Cephalosphaera* (Myristicaceae), with a replacement name, *Neobrochoneura*, and new combinations in this genus for Madagascan species previously included in *Brochoneura*. *Phytotaxa* 456: 299–300.

Fonseca, L. H. M., P. Asselman, K. R. Goodrich, F. J. Nge, V. Soulé, K. Mercier, et al. 2024. Truly the best of both worlds: merging lineage-specific and universal baiting kits to maximize phylogenomic inference. *Applications in Plant Sciences* 12: e11615.

Frost, L., D. A. Santamaría-Aguilar, D. Singletary, and L. P. Lagomarsino. 2022. Neotropical niche evolution of *Otoba* trees in the context of global biogeography of the nutmeg family. *Journal of Biogeography* 49: 156–170.

Guo, X., C. C. Tang, D. C. Thomas, T. L. P. Couvreur, and R. M. K. Saunders. 2017. A mega-phylogeny of the Annonaceae: taxonomic placement of five enigmatic genera and support for a new tribe, Phoenicantheae. *Scientific Reports* 7: 7323.

Hendriks, K. P., T. Mandáková, N. M. Hay, E. Ly, A. Hooft van Huysduynen, R. Tamrakar, S. K. Thomas, et al. 2021. The best of both worlds: Combining lineage-specific and universal bait sets in target-enrichment hybridization reactions. *Applications in Plant Sciences* 9: e11438.

Jaramillo, M. A., P. S. Manos, E. A. Zimmer, and E. Asia. 2004. Phylogenetic relationships of the perianthless Piperales: reconstructing the evolution of floral development. *International Journal of Plant Sciences* 165: 403–416.

Johnson, M. G., E. M. Gardner, Y. Liu, R. Medina, B. Goffinet, A. J. Shaw, N. J. C. Zerega, and N. J. Wickett. 2016. HybPiper: Extracting coding sequence and introns for phylogenetics from high-throughput sequencing reads using target enrichment. *Applications in Plant Sciences* 4: 1600016.

Johnson, M. G., L. Pokorny, S. Dodsworth, L. R. Botigué, R. S. Cowan, A. Devault, W. L. Eiserhardt, et al. 2019. A universal probe set for targeted sequencing of 353 nuclear genes from any flowering plant designed using k-medoids clustering. *Systematic Biology* 68: 594–606.

Jost, M., M.-S. Samain, I. Marques, S. W. Graham, and S. Wanke. 2021. Discordant phylogenomic placement of Hydnoraceae and Lactoridaceae within Piperales using data from all three genomes. *Frontiers in Plant Science* 12: 642598.

Junier, T., and E. M. Zdobnov. 2010. The Newick utilities: high-throughput phylogenetic tree processing in the Unix shell. *Bioinformatics* 26: 1669–1670.

Katoh, K., and D. M. Standley. 2013. MAFFT multiple sequence alignment software version 7: improvements in performance and usability. *Molecular Biology and Evolution* 30: 772–780.

Kühn, U., and K. Kubitzki. 1993. Myristicaceae. *In* K. Kubitzki, J. G. Rohwer, and V. Bittrich [eds.], The families and genera of vascular plants II, 457–467. Springer, Berlin, Germany.

Lanfear, R., P. B. Frandsen, A. M. Wright, T. Senfeld, and B. Calcott. 2017. PartitionFinder 2: new methods for selecting partitioned models of evolution for molecular and morphological phylogenetic analyses. *Molecular Biology and Evolution* 34: 772–773.

Larridon, I., T. Villaverde, A. R. Zuntini, L. Pokorny, G. E. Brewer, N. Epitawalage, I. Fairlie, et al. 2020. Tackling rapid radiations with targeted sequencing. *Frontiers in Plant Science* 10: 1655.

Li, H., and R. Durbin. 2009. Fast and accurate short read alignment with Burrows–Wheeler transform. *Bioinformatics* 25: 1754–1760.

Li, H., B. Liu, C. C. Davis, and Y. Yang. 2020. Plastome phylogenomics, systematics, and divergence time estimation of the *Beilschmiedia* group (Lauraceae). *Molecular Phylogenetics and Evolution* 151: 106901.

Li, H. T., Y. Luo, L. Gan, P. F. Ma, L. M. Gao, J. B. Yang, J. Cai, et al. 2021. Plastid phylogenomic insights into relationships of all flowering plant families. *BMC Biology* 19: 232.

Li, H. T., T. S. Yi, L. M. Gao, P. F. Ma, T. Zhang, J. B. Yang, M. A. Gitzendanner, et al. 2019. Origin of angiosperms and the puzzle of the Jurassic gap. *Nature Plants* 5: 461–470.

Lírio, E. J. de, A. L. Peixoto, P. T. Sano, and A. P. Moraes. 2020. Cytogenetics, geographic distribution, conservation, and a new species of *Macrotorus* (Mollinedioideae, Monimiaceae) from the Brazilian Atlantic Forest. *Systematic Botany* 45: 754–759.

Lírio, E. J. de, A. L. Peixoto, and M. F. De Siqueira. 2015. Taxonomy, conservation, geographic and potential distribution of *Macrotorus* Perkins (Mollinedioideae, Monimiaceae), and a key to the Neotropical genera of Monimiaceae. *Phytotaxa* 234: 201–214.

Magallón, S., S. Gómez-Acevedo, L. L. Sánchez-Reyes, and T. Hernández-Hernández. 2015. A metacalibrated time-tree documents the early rise of flowering plant phylogenetic diversity. *New Phytologist* 207: 437–453.

Massoni, J., J. Doyle, and H. Sauquet. 2015. Fossil calibration of Magnoliidae, an ancient lineage of angiosperms. *Palaeontologia Electronica* 18.1.2FC: 1–25.

Massoni, J., F. Forest, and H. Sauquet. 2014. Increased sampling of both genes and taxa improves resolution of phylogenetic relationships within Magnoliidae, a large and early-diverging clade of angiosperms. *Molecular Phylogenetics and Evolution* 70: 84–93.

McDonnell, A. J., W. J. Baker, S. Dodsworth, F. Forest, S. W. Graham, M. G. Johnson, L. Pokorny, et al. 2021. Exploring Angiosperms353: developing and applying a universal toolkit for flowering plant phylogenomics. *Applications in Plant Sciences* 9: e11443.

Michalak, I., L.-B. Zhang, and S. S. Renner. 2010. Trans-Atlantic, trans-Pacific and trans-Indian Ocean dispersal in the small Gondwanan Laurales family Hernandiaceae. *Journal of Biogeography* 37: 1214–1226.

Minh, B. Q., H. A. Schmidt, O. Chernomor, D. Schrempf, M. D. Woodhams, A. von Haeseler, and R. Lanfear. 2020. IQ-TREE 2: New models and efficient methods for phylogenetic inference in the genomic era. *Molecular Biology and Evolution* 37: 1530–1534.

Moore, M. J., C. D. Bell, P. S. Soltis, and D. E. Soltis. 2007. Using plastid genome-scale data to resolve enigmatic relationships among basal angiosperms. *Proceedings of the National Academy of Sciences, USA* 104: 19363–19368.

Naumann, J., K. Salomo, J. P. Der, E. K. Wafula, J. F. Bolin, E. Maass, L. Frenzke, et al. 2013. Single-copy nuclear genes place haustorial Hydnoraceae within Piperales and reveal a Cretaceous origin of multiple parasitic angiosperm lineages. *PLoS One* 8: e79204.

Nge, F. J., T. Chaowasku, A. Damthongdee, C. Wiya, V. R. C. Soulé, C. Rodrigues-Vaz, D. Bruy, et al. 2024. Complete genus-level phylogenomics and new subtribal classification of the pantropical plant family Annonaceae. *Taxon* 73: 1341–1369.

One Thousand Plant Transcriptomes Initiative. 2019. One thousand plant transcriptomes and the phylogenomics of green plants. *Nature* 574: 679–685.

Peixoto, A. L., and M. V. L. Pereira-Moura. 2008. A new genus of Monimiaceae from the Atlantic Coastal Forest in South-Eastern Brazil. *Kew Bulletin* 63: 137–141.

Philipson, W. R. 1987. A classification of the Monimiaceae. *Nordic Journal of Botany* 7: 25–29.

Philipson, W. R. 1988. A classification of the Monimiaceae—an additional note. *Nordic Journal of Botany* 8: 24.

Philipson, W. R. 1993. Monimiaceae. *In* K. Kubitzki, J. G. Rohwer, and V. Bittrich [eds.], The families and genera of vascular plants II, 426–437. Springer, Berlin, Germany.

Portik, D. M., and J. J. Wiens. 2021. Do alignment and trimming methods matter for phylogenomic (UCE) analyses? *Systematic Biology* 70: 440–462.

Qiu, Y.-L., J. H. Lee, F. Bernasconi-Quadroni, D. E. Soltis, P. S. Soltis, M. Zanis, E. A. Zimmer, et al. 1999. The earliest angiosperms: evidence from mitochondrial, plastid and nuclear genomes. *Nature* 402: 404–407.

Ramírez-Barahona, S., H. Sauquet, and S. Magallón. 2020. The delayed and geographically heterogeneous diversification of flowering plant families. *Nature Ecology & Evolution* 4: 1232–1238.

Renner, S. S., and A. S. Chanderbali. 2000. What is the relationship among Hernandiaceae, Lauraceae, and Monimiaceae, and why is this question so difficult to answer? *International Journal of Plant Sciences* 161: S109–S119.

Renner, S. S., J. S. Strijk, D. Strasberg, and C. Thébaud. 2010. Biogeography of the Monimiaceae (Laurales): a role for East Gondwana and long-distance dispersal, but not West Gondwana. *Journal of Biogeography* 37: 1227–1238.

Rohwer, J. G. 2000. Toward a phylogenetic classification of the Lauraceae: evidence from *matK* sequences. *Systematic Botany* 25: 60–71.

Samain, M. S., G. Mathieu, S. Wanke, C. Neinhuis, and P. Goetghebeur. 2008. *Verhuellia* revisited—unravelling its intricate taxonomic history and a new subfamilial classification of Piperaceae. *Taxon* 57: 583–587.

Sauquet, H. 2003. Androecium diversity and evolution in Myristicaceae (Magnoliales), with a description of a new Malagasy genus, *Doyleanthus* gen. nov. *American Journal of Botany* 90: 1293–1305.

Sauquet, H. 2004. Systematic revision of Myristicaceae (Magnoliales) in Madagascar, with four new species of *Mauloutchia*. *Botanical Journal of the Linnean Society* 146: 351–368.

Sauquet, H., M. von Balthazar, J. A. Doyle, P. K. Endress, S. Magallón, Y. Staedler, and J. Schönenberger. 2018. Challenges and questions in reconstructing the ancestral flower of angiosperms: a reply to Sokoloff et al. *American Journal of Botany* 105: 127–135.

Sauquet, H., M. von Balthazar, S. Magallón, J. A. Doyle, P. K. Endress, E. J. Bailes, E. Barroso de Morais, et al. 2017. The ancestral flower of angiosperms and its early diversification. *Nature Communications* 8: 16047.

Sauquet, H., J. A. Doyle, T. Scharaschkin, T. Borsch, K. W. Hilu, L. W. Chatrou, and A. Le Thomas. 2003. Phylogenetic analysis of Magnoliales and Myristicaceae based on multiple data sets: implications for character evolution. *Botanical Journal of the Linnean Society* 142: 125–186.

Sayyari, E., J. B. Whitfield, and S. Mirarab. 2018. DiscoVista: interpretable visualizations of gene tree discordance. *Molecular Phylogenetics and Evolution* 122: 110–115.

Shah, T., J. V Schneider, G. Zizka, O. Maurin, W. Baker, F. Forest, G. E. Brewer, et al. 2021. Joining forces in Ochnaceae phylogenomics: a tale of two targeted sequencing probe kits. *American Journal of Botany* 108: 1201–1216.

Slater, G. S. C., and E. Birney. 2005. Automated generation of heuristics for biological sequence comparison. *BMC Bioinformatics* 6: 31.

Smirnov, V., and T. Warnow. 2021. MAGUS: Multiple sequence Alignment using Graph clUStering. *Bioinformatics* 37: 1666–1672.

Smith, J., A. Stevens, E. Tepe, and C. Davidson. 2008. Placing the origin of two species-rich genera in the late Cretaceous with later species divergence in the Tertiary: a phylogenetic, biogeographic and molecular dating analysis of *Piper* and *Peperomia* (Piperaceae). *Plant Systematics and Evolution* 275: 9–30.

Smith, M. R. 2022. Robust analysis of phylogenetic tree space. *Systematic Biology* 71: 1255–1270.

Soltis, D. E., S. A. Smith, N. Cellinese, K. J. Wurdack, D. C. Tank, S. F. Brockington, N. F. Refulio-Rodriguez, et al. 2011. Angiosperm phylogeny: 17 genes, 640 taxa. *American Journal of Botany* 98: 704–730.

Song, Y., W.-B. Yu, Y.-H. Tan, J.-J. Jin, B. Wang, J.-B. Yang, B. Liu, and R. T. Corlett. 2020. Plastid phylogenomics improve phylogenetic resolution in the Lauraceae. *Journal of Systematics and Evolution* 58: 423–439.

Stamatakis, A. 2014. RAxML version 8: a tool for phylogenetic analysis and post-analysis of large phylogenies. *Bioinformatics* 9: 1312–1313.

Stevens, P. F. 2022. Angiosperm phylogeny website, version 14, July 2017 [and more or less continuously updated since]. Website: http://www.mobot.org/MOBOT/research/APweb/

Thomas, D. C., L. W. Chatrou, G. W. Stull, D. M. Johnson, D. J. Harris, U. Thongpairoj, and R. M. K. Saunders. 2015. The historical origins of palaeotropical intercontinental disjunctions in the pantropical flowering plant family Annonaceae. *Perspectives in Plant Ecology, Evolution and Systematics* 17: 1–16.

Wanke, S., M. A. Jaramillo, T. Borsch, M.-S. Samain, D. Quandt, and C. Neinhuis. 2007a. Evolution of Piperales—*matK* gene and *trnK* intron sequence data reveal lineage specific resolution contrast. *Molecular Phylogenetics and Evolution* 42: 477–497.

Wanke, S., L. Vanderschaeve, G. Mathieu, C. Neinhuis, P. Goetghebeur, and M. S. Samain. 2007b. From forgotten taxon to a missing link? The position of the genus *Verhuellia* (Piperaceae) revealed by molecules. *Annals of Botany* 99: 1231–1238.

Wickett, N. J., S. Mirarab, N. Nguyen, T. Warnow, E. Carpenter, N. Matasci, S. Ayyampalayam, et al. 2014. Phylotranscriptomic analysis of the origin and early diversification of land plants. *Proceedings of the National Academy of Sciences, USA* 111: E4859–E4868.

Zhang, C., M. Rabiee, E. Sayyari, and S. Mirarab. 2018. ASTRAL-III: polynomial time species tree reconstruction from partially resolved gene trees. *BMC Bioinformatics* 19: 153.

Zuntini, A. R., T. Carruthers, O. Maurin, P. C. Bailey, K. Leempoel, G. E. Brewer, N. Epitawalage, et al. 2024. Phylogenomics and the rise of the angiosperms. *Nature* 629: 843–850.

SUPPORTING INFORMATION

Additional supporting information can be found online in the Supporting Information section at the end of this article.

Appendix S1. Full voucher and source information for all taxa included in this study.

Appendix S2. Lengths of loci recovered and those used in analyses. Panel (a) is a density plot showing the distribution of the mean length of exon recovered for each of the 353 exons in the data set. The bottom two panels show the distribution of lengths of each (b) exon and (c) supercontig (exon plus off-target intron sequence data) after it has been aligned and trimmed (using the methods to produce the tree in Figures 4 and 5). Dotted vertical lines indicate the mean length, and a rug plot showing each individual length measurement is found under the densities.

Appendix S3. Venn diagram showing how loci that are selected as suitable for phylogenetic inference for each order are shared among orders. Filtering was conducted on each order separately to generate the set of loci for which at least 50% of the exon was recovered in at least 50% of specimens ($l = 50\%$, $i = 50\%$). The number of loci is shown in each section of the Venn diagram. For example, the central section indicates that there are 52 loci that are recovered well enough to be selected as suitable for phylogenetic inference in each of the five orders. In another contrasting example, 18 loci were only suitable for phylogenetic inference in Canellales under this filtering.

Appendix S4. Coalescent tree from Figure 5 (with branch lengths removed) alongside a heatmap showing the proportion of exon recovered for all 353 exons in the Angiosperms353 kit.

Appendix S5. Density plots showing the distributions of (a) mean linear posterior probability (LPP) and (b) mean quartet score (QS) for each ASTRAL tree in this study (see tables in Appendix S10 for details of trees). Each plot is split into two overlapping densities representing support metrics at shallow (node depth <5) and deep (node depth ≥5) branches.

Appendix S6. Phylogenetic relationships in magnoliids obtained in our main coalescent analysis (same tree as Figures 4, 5).

Appendix S7. Phylogenetic relationships in magnoliids obtained in our main concatenation analysis. Pie charts at nodes represent bootstrap support values for associated branches. Branches are in units of substitutions per site with a scale bar in the bottom left.

Appendix S8. Tanglegram detailing topological differences between the main coalescent (left; Figures 4, 5; Appendix S6) and concatenation (right; Appendix S7) analyses. Grey dashed lines join the corresponding tips in each tree. Branch lengths were removed from the coalescent tree for ease of interpretation.

Appendix S9. Tanglegram detailing topological differences between the main coalescent tree (left; Figures 4, 5) and a tree constructed using the same analytical approach but without 18 samples that had poor recoveries (right). Branch lengths were removed.

Appendix S10. Tables summarizing the effect of different analytical choices on four support metrics: normalized scores, total number of quartets, mean local posterior probability across all nodes (LPP) and mean quartet support across all nodes (QS). These metrics were standardized and summed to provide a support "score" for each tree (scaled sum). The analysis highlighted in boldface received the highest sum of scaled values across four quality metrics and was used as our main reference analysis presented in this paper (Figures 4, 5).

Appendix S11. Heatmap showing how the strength of support for major clades (families, orders) across coalescent analyses from a range of different analytical approaches. Strong/weak support indicates whether the relevant branch of the gene tree had a local posterior probability (LPP) support value above/below a threshold of 0.9. Weakly rejected clades correspond to clades that are not present in the tree, but are compatible if low support branches (below 0.9 LPP) are contracted. If they are still not compatible, they count as strongly rejected clades.

Appendix S12. Stacked bar plots showing the number of gene trees that support the monophyly of major magnoliid clades (as in Appendix S11). The set of gene trees used were the same as those used for the tree in Figure 5. Strong/weak support indicates whether the relevant branch of the gene tree had a bootstrap support value above/below a threshold of 90%. Weakly rejected clades are those that are not in the tree but are compatible if low support branches (below 75%) are contracted. Those branches that were not compatible after contracting low support branches count as a strong rejection. Note that if one species or subclade is missing in a gene tree, the clade will be considered missing.

Appendix S13. Heatmap depicting the Robinson-Foulds distances between pairs of trees generated by our analyses.

Appendix S14. Pairwise scatterplots of the four different support metrics used in our study. Each point represents an ASTRAL tree (as listed in Appendix S10). Mean LPP and QS refer to the average local posterior probability and quartet support across all branches in the tree, respectively.

How to cite this article: Helmstetter, A. J., Z. Ezedin, E. J. de Lírio, S. M. de Oliveira, L. W. Chatrou, R. H. J. Erkens, I. Larridon, et al. 2025. Toward a phylogenomic classification of magnoliids. *American Journal of Botany* 111: e16451. https://doi.org/10.1002/ajb2.16451

Appendix 1. Taxonomic treatment.

Meiocarpidieae Chatrou, Couvreur & Erkens, tribus nov., based on Meiocarpidioideae Chaowasku, Acta Bot. Brasil. 34(3): 525 (2020).

Type: *Meiocarpidium* Engl. & Diels

Note: See Chaowasku (2020) for details about morphological characterization of the tribe.

Mauloutchieae Ezedin & Sauquet, tribus nov.

Type: *Mauloutchia* Warb.

Description: Middle to high canopy trees or very rarely lianas (*Pycnanthus* spp.); dioecious or monoecious. **Sap** reddish to brownish or yellowish then oxidizing red. **Leaves** abaxially glaucous (*Cephalosphaera* and *Pycnanthus*) or not, papillose hairs absent or present and often early glabrescent, dots absent or rarely present (*Staudtia*); vernation convolute, lines sometimes present. **Inflorescences** dense globose cyme (*Staudtia*) or panicle (the rest). **Flowers** unisexual; perianth 3–4(–5)-merous, green-yellow to orangish-red, spreading or reflexed at anthesis; synandrium stalk terete and convex, exserted or inserted but not completely enclosed by the perianth lobes (*Brochoneura* and *Doyleanthus*), unbranched monocyclic or branched (*Mauloutchia*), when branched with or without distinct phyllotaxy, anthers 3–5(–60), fused to the synandrium column or basifixed and free when branched. **Pollen** globose to boat shaped, aperture ulcerate or sulcate, exine sculpturing continuous to granulately verrucate-rugulate or minutely reticulate with psilate spines (*Pycnanthus*). **Fruits** dehiscent, globose to ellipsoid, glabrous or glabrescent, greenish to orangish-brown; pericarp thin (*Cephalosphaera*) to thick (*Pycnanthus*), smooth to slightly ridged or rarely carinate (*M. chapelieri*), leathery. **Arils** rudimentary to well developed or absent (*Mauloutchia*), when present partly enclosing the seed or rarely entire (*Staudtia*), deeply laciniate or only near apex (*Staudtia*), opaque creamy white (*Cephalosphaera*) to deep red (*Staudtia*). **Seeds** ellipsoid to ovoid; albumen not ruminate (except in *Pycnanthus*), containing oil.

Genera included: *Cephalosphaera* Warb. (1), *Doyleanthus* Sauquet (1), *Mauloutchia* Warb. (9), *Brochoneura* Warb. (3), *Pycnanthus* Warb. (4), and *Staudtia* Warb. (2–3).

Notes: This tribe displays the widest array of diversity across several traits, making it difficult to characterize morphologically. In particular, there is high diversity in anther morphology when compared to the remainder of the family, especially for *Mauloutchia*, where the synandrium is branched, often with distinct phyllotaxy, and with basifixed anthers, which is unique in the family (Sauquet, 2004). The only other genus in which a non-entire synandrium can be found is in a few species of *Knema* with lobed synandria. Monoecy is widespread in the tribe, whereas dioecy appears randomly, specifically in *Brochoneura* and *Pycnanthus* which have been observed to contain individuals that are either dioecious or monoecious (Kühn and Kubitzki, 1993; Sauquet et al., 2003). Endosperm rumination is largely absent in this tribe, being only present in *Pycnanthus* (Kühn and Kubitzki, 1993), which would suggest ruminations as being derived in the family and having evolved more than once. *Doyleanthus* has yet to be sampled in a molecular analysis; however, its morphology strongly suggests placement near the *Brochoneura*–*Mauloutchia* clade (Sauquet, 2003). Figueiredo and Smith (2020) argued that *Brochoneura* should be used for the type and single species of the East African genus *Cephalosphaera* and erected *Neobrochoneura* to accommodate the Malagasy species of *Brochoneura*. However, we believe this change is confusing and have proposed to conserve the names *Brochoneura* and *Cephalosphaera* (Ezedin and Sauquet, 2024).

Scyphocephalieae Ezedin & Sauquet, tribus nov.

Type: *Scyphocephalium* Warb.

Description: High canopy trees; dioecious. **Sap** red. **Leaves** abaxially not glaucous, hairs rusty ferruginous and persistent, dots present; vernation convolute. **Inflorescences** dense globose cyme, sessile or pedunculate, in up to three heads, each head subtended by 2 bracts. **Flowers** unisexual; perianth (3–)4–5-merous, pinkish red, spreading at anthesis; synandrium stalk terete and flat-topped, inserted, unbranched monocyclic, anthers 6–10, fused to the synandrium column. **Pollen** boat shaped, aperture ulcerate, exine sculpturing reticulate with muri subunits triangular and forming a crotonoid pattern. **Fruits** indehiscent, irregular globose, pubescent, orangish brown; pericarp fleshy. **Arils** entire. **Seeds** flattened; albumen ruminate, containing oil.

Genera included: *Scyphocephalium* Warb. (2).

Notes: Much remains unknown regarding the enigmatic *Scyphocephalium*. Possible synapomorphies include inflorescences of pedunculate cymes bearing densely globose heads, pollen exine sculpturing in triangular crotonoid pattern, fruits indehiscent, and seeds flattened.

Horsfieldieae Ezedin & Sauquet, tribus nov.

Type: *Horsfieldia* Willd.

Description: Shrubs to mid canopy trees; dioecious or monoecious (*Endocomia*). **Sap** orange-reddish. **Leaves** abaxially glaucous or not, papillose hairs absent or rarely present (*H. iryaghedhi*), dots absent or rarely present (*Horsfieldia* spp.); vernation conduplicate. **Inflorescences** paniculate with caducous basal cataphylls, bracts small or large and caducous, terminal buds absent. **Flowers** unisexual; perianth (2–)3–4(–5)-merous, green to orange, barely open or spreading to slightly recurved at anthesis; synandrium stalk terete and concave (rarely convex in *Endocomia*); anthers (2–)5–20(–30), fused to the synandrium column; ovary ovoid (rarely ovoid-ellipsoid in *Horsfieldia*), glabrous or pubescent; stigma usually small, narrow or broad, 2-lobed, each lobe entire or (2–)3–5(–6)-lobulate. **Pollen** boat shaped, aperture sulcate, exine sculpturing often reticulate or rarely rugulate (*Gymnacranthera*). **Fruits** dehiscent, globose to ellipsoid, glabrescent to pubescent (rarely glabrous in *Horsfieldia* spp.), greenish-yellow to dark orange; pericarp often thick leathery or somewhat fleshy, with or without tubercles, perianth sometimes persistent (*Horsfieldia*). **Arils** well developed, entire or shallowly (*Horsfieldia* spp.) to deeply (*Gymnacranthera*) laciniate, yellowish to red. **Seeds** ellipsoid, pointed at the apex (in *Endocomia*) or not, variegated (in *Endocomia*) or not; albumen ruminate, containing oil, starch absent; cotyledons divaricate, connate at base.

Genera included: *Endocomia* W.J. de Wilde (4), *Gymnacranthera* (A. DC.) Warb. (7), and *Horsfieldia* Willd. (106).

Notes: Possible synapomorphies for this clade include inflorescences subtended with basal cataphyll scars and seeds containing oil but no starch.

Myristiceae Ezedin & Sauquet, tribus nov.

Type: *Myristica* Gronov.

Description: Subcanopy to mid canopy trees; dioecious. **Sap** orangish-reddish or clear then oxidizing orange-red. **Leaves** abaxially glaucous or not, papillate hairs absent or sometimes present (*Myristica* spp.), dots present or absent; vernation conduplicate. **Inflorescences** short-branched paniculate or short wart-like, continuously growing woody brachyblasts from which flowers are successively borne, lacking basal cataphylls, bracteoles minute and caducous. **Flowers** unisexual; perianth (2–)3–4(–5)-merous, yellowish to reddish-brown, spreading and reflexed at anthesis; synandrium stalk terete and convex (*Myristica*) or concave (*Paramyristica*), flattened into a disk (*Knema*), inserted or rarely exserted (*Knema* spp.), unbranched monocyclic or rarely sublobate and whorled (i.e., *K. celebica*), anthers (3–)9–25(–30), fused to the synandrium column; ovary subglobose to oblong (rarely fusiform), pubescent; stigma often minutely 2-lobed, each lobe (2–)3–5(–6)-lobulate (in *Knema*). **Pollen** boat shaped (*Knema*) or elliptical and approaching boat shaped (*Myristica*), aperture sulcate, exine sculpturing reticulate to rugulate. **Fruits** dehiscent, globose to ellipsoid, glabrescent or pubescent (rarely glabrous in *Myristica* spp.), light greenish-yellow to orange; pericarp smooth, thick and fleshy (*Myristica*) or leathery (*Knema*). **Arils** well developed, laciniate completely or partly so to the base (*Myristica*) or entire and rarely laciniate at the apex only (*Knema*), yellow to deep red. **Seeds** ellipsoid, not variegated; albumen ruminate, containing oil and starch; cotyledons divaricate or rarely suberect (*Knema* spp.), connate at base and edges (*Myristica*) or very slightly to rarely so (*Knema*).

Genera included: *Knema* Lour. (96), *Myristica* Gronov. (173), and *Paramyristica* W.J. de Wilde (1).

Notes: The close relationship between *Myristica* and *Knema* is well supported in molecular analyses. Although dioecious, a few individuals of *Myristica* have been reported as monoecious by de Wilde (1984) who considered these cases anomalous. *Paramyristica* is tentatively included here based on morphological grounds and partly from the results of our phylogenetic analyses; however, its topological placement remains unstable. Possible synapomorphies for this clade are inflorescences lacking basal cataphyll scars and seeds containing oil and starch. *Paramyristica* notably deviates from the tribe as it has cataphyll scars and lacks bracteoles (de Wilde, 1994).

Viroleae S.M. Oliveira & Sauquet, tribus nov.

Type: *Virola* Aubl.

Description: Mid to high canopy trees or very rarely shrubs (*Virola sessilis* and *V. subsessilis*); dioecious or rarely monoecious (*Iryanthera* spp.). **Sap** red, brownish, pinkish, sometimes initially watery then oxidizing opaque white (*Otoba* spp.) or straw-colored (*Osteophloeum*). **Leaves** with persistent indument or glabrescent; hairs sessile stellate, dendritic, stipitate stellate or malpighiaceous (*Iryanthera* spp.); vernation convolute or conduplicate (*Otoba*), lines sometimes present. **Inflorescences** axillary, supra axillary or less often cauliflorous (*Iryanthera* spp.), racemose or variously branched paniculate; bracts mostly caducous; bracteoles present or not. **Flowers** unisexual; perianth 3–4(−5)-merous, 1-4 cm long, partly connate, often fleshy, yellow or slightly green to whitish; synandrium stalk terete, flat to convex; anthers 2–10(−20), fused to the synandrium column or free and basifixed (in *Compsoneura* spp., *Otoba* spp.), dehiscing by longitudinal slits; ovary sessile or short stipitate, globose, subglobose, ovoid, ellipsoid or pyriform, glabrous or pubescent, unicarpellate, unilocular; stigma sessile, 2-lobed. **Pollen** in monads or exceptionally tetrads (*Iryanthera*); size 21–40 μm; mostly sulcate with sharply delimited aperture or sulcoidate with aperture not sharply defined; boat shaped or globose spherical; exine sculpturing reticulate or psilate (*Otoba*). **Fruits** dehiscent, 2-valvate, globose, subglobose or ellipsoid, glabrous, glabrescent or pubescent. **Arils** partly to completely enclosing the seed, red, opaque orangish-red or translucent white (*Otoba* spp.). **Seeds** ellipsoid, variegated (in *Compsoneura*) or not; albumen ruminate, containing oil; cotyledons often vestigial, divergent, and becoming haustorial during germination.

Genera included: *Bicuiba* W.J. de Wilde (1), *Compsoneura* (DC.) Warb. (18), *Iryanthera* (A. DC.) Warb. (22), *Osteophloeum* Warb. (1), *Otoba* (DC.) H. Karst. (12), and *Virola* Aubl. (71).

Notes: Outside of Mauloutchieae, this tribe contains the only other two genera which contain species that exhibit basifixed and free anthers: *Compsoneura* and *Otoba*.